

---

# Exploring the Influence of Information Entropy Change in Learning Systems

---

**Xiaowei Yu**  
CSE  
UT-Arlington

**Yao Xue**  
ERP  
Southern Illinois University

**Lu Zhang**  
CSE  
UT-Arlington

**Li Wang**  
Department of Mathematics  
UT-Arlington

**Tianming Liu**  
School of Computing  
University of Georgia

**Dajiang Zhu**  
CSE  
UT-Arlington

## Abstract

In this work, we explore the influence of entropy change in deep learning systems by adding noise to the inputs/latent features. The applications in this paper focus on deep learning tasks within computer vision, but the proposed theory can be further applied to other fields, such as natural language processing (NLP). Noise is conventionally viewed as a harmful perturbation in various deep learning architectures, such as convolutional neural networks (CNNs) and vision transformers (ViTs), as well as different learning tasks like image classification and transfer learning. However, this work aims to rethink whether the conventional proposition always holds. We demonstrate that specific noise can boost the performance of various deep architectures under certain conditions. We theoretically prove the enhancement gained from positive noise by reducing the task complexity defined by information entropy and experimentally show the significant performance gain in large image datasets, such as the ImageNet. Herein, we use the information entropy to define the complexity of the task. We categorize the noise into two types, positive noise (PN) and harmful noise (HN), based on whether the noise can help reduce the complexity of the task. Extensive experiments of CNNs and ViTs have shown performance improvements by proactively injecting positive noise, where we achieve an unprecedented top 1 accuracy over 95% on ImageNet. Both theoretical analysis and empirical evidence have confirmed that the presence of positive noise, can benefit the learning process, while the traditionally perceived harmful noise indeed impairs deep learning models. The different roles of noise offer new explanations for deep models on specific tasks and provide a new paradigm for improving model performance. Moreover, it reminds us that we can influence the performance of learning systems via information entropy change.

## 1 Introduction

Noise, conventionally regarded as a hurdle in machine learning and deep learning tasks, is universal and unavoidable due to various reasons, e.g., environmental factors, instrumental calibration, and human activities [39] [57]. In computer vision, noise can be generated from different phases: (1) Image Acquisition: Noise can arise from a camera sensor or other imaging device [52]. For example, electronic or thermal noise in the camera sensor can result in random pixel values or color variations that can be visible in the captured image. (2) Image Preprocessing: Noise can be introduced during preprocessing steps such as image resizing, filtering, or color space conversion [1]. For example, resizing an image can introduce aliasing artifacts, while filtering an image can result in the loss of

detail and texture. (3) Feature Extraction: Feature extraction algorithms can be sensitive to noise in the input image, which can result in inaccurate or inconsistent feature representations [2]. For example, edge detection algorithms can be affected by noise in the image, resulting in false positives or negatives. (4) Algorithms: algorithms used for computer vision tasks, such as object detection or image segmentation, can also be sensitive to noise in the input data [6]. Noise can cause the algorithm to learn incorrect patterns or features, leading to poor performance.

Since noise is an unavoidable reality in engineering tasks, existing works usually make the assumption that noise has a consistently negative impact on the current task [47] [40]. Nevertheless, is the above assumption always valid? As such, it is crucial to address the question of whether noise can ever have a positive influence on deep learning models. This work aims to provide a comprehensive answer to this question, which is a pressing concern in the deep learning community. We recognize that the imprecise definition of noise is a critical factor leading to the uncertainties surrounding the identification and characterization of noise. To address these uncertainties, an in-depth analysis of the task’s complexity is imperative for arriving at a rigorous answer. By using the definition of task entropy, it is possible to categorize noise into two distinct categories: positive noise (PN) and harmful noise (HN). PN decreases the complexity of the task, while HN increases it, aligning with the conventional understanding of noise.

## 1.1 Scope and Contribution

Our work aims to investigate how various types of noise affect deep learning models. Specifically, the study focuses on three common types of noise, i.e., Gaussian noise, linear transform noise, and salt-and-pepper noise. Gaussian noise refers to random fluctuations that follow a Gaussian distribution in pixel values at the image level or latent representations in latent space [46]. Linear transforms, on the other hand, refer to affine elementary transformations to the dataset of original images or latent representations, where the transformation matrix is row equivalent to an identity matrix [56]. Salt-and-pepper noise is a kind of image distortion that adds random black or white values at the image level or to the latent representations [7].

This paper analyzes the impact of these types of noise on the performance of deep learning models for image classification and domain adaptation tasks. Two popular model families, Vision Transformers (ViTs) and Convolutional Neural Networks (CNNs), are considered in the study. Image classification is one of the most fundamental tasks in computer vision, where the goal is to predict the class label of an input image. Domain adaptation is a practically meaningful task where the training and test data come from different distributions, also known as different domains. By investigating the effects of different types of noise on ViTs and CNNs for typical deep learning tasks, the paper provides insights into the influences of noises on deep models. The findings presented in this paper hold practical significance for enhancing the performance of various types of deep learning models in real-world scenarios.

The contributions of this paper are summarized as follows:

- We re-examined the conventional view that noise, by default, has a negative impact on deep learning models. Our theoretical analysis and experimental results show that noise can be a positive support for deep learning models and tasks.
- We implemented extensive experiments with different deep models, such as CNNs and ViTs, and on different deep learning tasks. Empowered by positive noise, we achieved state-of-the-art (SOTA) results in all the experiments presented in this paper.
- Instead of operating on the image level, our injecting noise operations are performed in the latent space. We theoretically analyze the difference between injecting noise on the image level and in the latent space.
- The theory and framework of reducing task complexity via positive noise in this work can be applied to any deep learning architecture. There is great potential for exploring the application of positive noise in other deep-learning tasks beyond the image classification and domain adaptation tasks examined in this study.

## 1.2 Related Work

**Positive Noise** In fact, within the signal-processing society, it has been demonstrated that random noise helps stochastic resonance improve the detection of weak signals [4]. Noises can have positive support and contribute to less mean square error compared to the best linear unbiased estimator when the mixing probability distribution is not in the extreme region [44]. Also, it has been reported that noise could increase the model generalization in natural language processing (NLP) [43]. Recently, the perturbation, a special case of positive noise, has been effectively utilized to implement self-refinement in domain adaptation and achieved state-of-the-art performance [56]. The latest research shows that by proactively adding specific noise to partial datasets, various tasks can benefit from the positive noise [29]. Besides, noises are found to be able to boost brain power and be useful in many neuroscience studies [36] [38].

**Deep Model** Convolutional Neural Networks have been widely used for image classification, object detection, and segmentation tasks, and have achieved impressive results [27] [21]. However, these networks have limitations in terms of their ability to capture long-range dependencies and extract global features from images. Recently, Vision Transformers has been proposed as an alternative to CNNs [15]. ViT relies on self-attention mechanisms and a transformer-based architecture to enable global feature extraction and modeling of long-range dependencies in images [60]. The attention mechanism allows the model to focus on the most informative features of the input image, while the transformer architecture facilitates information exchange between different parts of the image. ViT has demonstrated impressive performance on a range of image classification tasks and has the potential to outperform traditional CNN-based approaches. However, ViT currently requires a large number of parameters and training data to achieve state-of-the-art results, making it challenging to implement in certain settings [67].

## 2 Preliminary

In information theory, the entropy [49] of a random variable  $x$  is defined as:

$$H(x) = \begin{cases} -\int p(x) \log p(x) dx & \text{if } x \text{ is continuous} \\ -\sum_x p(x) \log p(x) & \text{if } x \text{ is discrete} \end{cases} \quad (1)$$

where  $p(x)$  is the distribution of the given variable  $x$ . The mutual information (MI) of two random discrete variables  $(x, y)$  is denoted as [9]:

$$\begin{aligned} MI(x, y) &= D_{KL}(p(x, y) \parallel p(x) \otimes p(y)) \\ &= H(x) - H(x|y) \end{aligned} \quad (2)$$

where  $D_{KL}$  is the Kullback–Leibler divergence [25], and  $p(x, y)$  is the joint distribution. The conditional entropy is defined as:

$$H(x|y) = -\sum p(x, y) \log p(x|y) \quad (3)$$

The above definitions can be readily expanded to encompass continuous variables through the substitution of the sum operator with the integral symbol. In this work, the noise is denoted by  $\epsilon$  if without any specific statement.

Before delving into the correlation between task and noise, it is imperative to address the initial crucial query of the mathematical measurement of a task  $\mathcal{T}$ . With the assistance of information theory, the complexity associated with a given task  $\mathcal{T}$  can be measured in terms of the entropy of  $\mathcal{T}$ . Therefore, we can borrow the concepts of information entropy to explain the difficulty of the task. For example, a smaller  $H(\mathcal{T})$  means an easier task and vice versa.

Since the entropy of task  $\mathcal{T}$  is formulated, it is not difficult to define the mutual information of task  $\mathcal{T}$  and noise  $\epsilon$  [29],

$$MI(\mathcal{T}, \epsilon) = H(\mathcal{T}) - H(\mathcal{T}|\epsilon) \quad (4)$$

Formally, if the noise can help reduce the complexity of the task, i.e.,  $H(\mathcal{T}|\epsilon) < H(\mathcal{T})$  then the noise has positive support. Therefore, a noise  $\epsilon$  is defined as **positive noise** (PN) when the noise satisfies  $MI(\mathcal{T}, \epsilon) > 0$ . On the contrary, when  $MI(\mathcal{T}, \epsilon) \leq 0$ , the noise is considered as the conventional

noise and named **harmful noise** (HN). The positive noise can be perceived as an augmentation of information gain brought by  $\epsilon$ .

$$\begin{cases} MI(\mathcal{T}, \epsilon) > 0 & \epsilon \text{ is positive noise} \\ MI(\mathcal{T}, \epsilon) \leq 0 & \epsilon \text{ is harmful noise} \end{cases} \quad (5)$$

**Moderate Model Assumption:** The positive noise may not work for deep models with severe problems. For example, the model is severely overfitting where models begin to memorize the random fluctuations in the data instead of learning the underlying patterns. In that case, the presence of positive noise will not have significant positive support in improving the models' performance. Besides, when the models are corrupted under brute force attack, the positive noise also can not work.

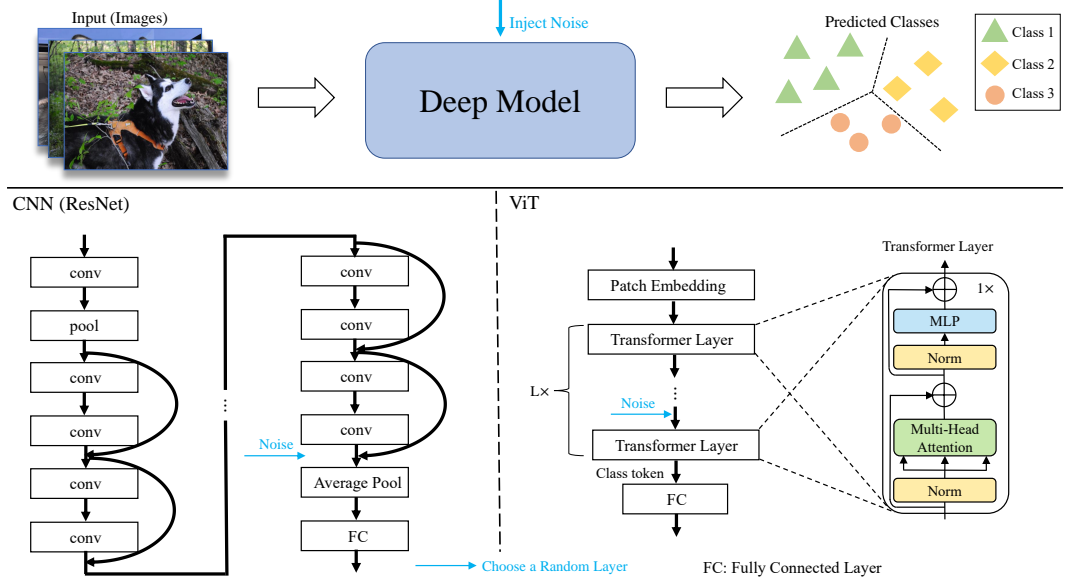


Figure 1: An overview of the proposed method. Above the black line is the standard pipeline for image classification. The deep model can be CNNs or ViTs. The noise is injected into a randomly chosen layer of the model represented by the blue arrow.

### 3 Methods

The idea of exploring the influence of noise on the deep models is straightforward. The framework is depicted in Fig. 1. This is a universal framework where there are different options for deep models, such as CNNs and ViTs. Through the simple operation of injecting noise into a randomly selected layer, a model has the potential to gain additional information to reduce task complexity, thereby improving its performance. It is sufficient to inject noise into a single layer instead of multiple layers since it imposes a regularization on multiple layers simultaneously.

For a classification problem, the dataset  $(\mathbf{X}, \mathbf{Y})$  can be regarded as samplings derived from  $D_{\mathcal{X}, \mathcal{Y}}$ , where  $D_{\mathcal{X}, \mathcal{Y}}$  is some unknown joint distribution of data points and labels from feasible space  $\mathcal{X}$  and  $\mathcal{Y}$ , i.e.,  $(\mathbf{X}, \mathbf{Y}) \sim D_{\mathcal{X}, \mathcal{Y}}$  [48]. Hence, given a set of  $k$  data points  $\mathbf{X} = \{X_1, X_2, \dots, X_k\}$ , the label set  $\mathbf{Y} = \{Y_1, Y_2, \dots, Y_k\}$  is regarded as sampling from  $\mathbf{Y} \sim D_{\mathcal{Y}|\mathcal{X}}$ . The complexity of  $\mathcal{T}$  on dataset  $\mathbf{X}$  is formulated as [29]:

$$H(\mathcal{T}; \mathbf{X}) = - \sum_{\mathbf{Y} \in \mathcal{Y}} p(\mathbf{Y}|\mathbf{X}) \log p(\mathbf{Y}|\mathbf{X}) \quad (6)$$

or

$$H(\mathcal{T}; \mathbf{X}) = H(\mathbf{Y}; \mathbf{X}) - H(\mathbf{X}) \quad (7)$$

The operation of adding noise at the image level can be formulated as:

$$\begin{cases} H(\mathcal{T}; \mathbf{X} + \epsilon) = -\sum_{\mathbf{Y} \in \mathcal{Y}} p(\mathbf{Y}|\mathbf{X} + \epsilon) \log p(\mathbf{Y}|\mathbf{X} + \epsilon) & \epsilon \text{ is additive noise} \\ H(\mathcal{T}; \mathbf{X}\epsilon) = -\sum_{\mathbf{Y} \in \mathcal{Y}} p(\mathbf{Y}|\mathbf{X}\epsilon) \log p(\mathbf{Y}|\mathbf{X}\epsilon) & \epsilon \text{ is multiplicative noise} \end{cases} \quad (8)$$

While the operation of proactively injecting noise in the latent space can be formulated as:

$$\begin{cases} H(\mathcal{T}; \mathbf{X} + \epsilon) := H(\mathbf{Y}; \mathbf{X} + \epsilon) - H(\mathbf{X}) & \epsilon \text{ is additive noise} \\ H(\mathcal{T}; \mathbf{X}\epsilon) := H(\mathbf{Y}; \mathbf{X}\epsilon) - H(\mathbf{X}) & \epsilon \text{ is multiplicative noise} \end{cases} \quad (9)$$

The formula 9 differs from the conventional definition of conditional entropy, as our method injects the noise into the latent representations instead of the original images. The Gaussian noise is additive, the linear transform noise is also additive, and the salt-and-pepper is a multiplicative noise.

**Gaussian Noise** The Gaussian noise is one of the most common additive noises that appear in computer vision tasks. The Gaussian noise is independent and stochastic, obeying the Gaussian distribution. Without loss of generality, defined as  $\mathcal{N}(\mu, \sigma^2)$ . Since our injection happens in the latent space, therefore, the complexity of the task is:

$$H(\mathcal{T}; \mathbf{X} + \epsilon) = H(\mathbf{Y}; \mathbf{X} + \epsilon) - H(\mathbf{X}). \quad (10)$$

We assume that both  $\mathbf{X}$  and  $\mathbf{Y}$  follow a multivariate normal distribution. Additionally, we can transform the distributions of  $\mathbf{X}$  and  $\mathbf{Y}$  to make them (approximately) follow the multivariate normal distribution, even if they initially do not [5] [17]. According to the definition in Equation 4, the mutual information with Gaussian noise is:

$$\begin{aligned} MI(\mathcal{T}, \epsilon) &= H(\mathbf{Y}; \mathbf{X}) - H(\mathbf{X}) - (H(\mathbf{Y}; \mathbf{X} + \epsilon) - H(\mathbf{X})) \\ &= H(\mathbf{Y}; \mathbf{X}) - H(\mathbf{Y}; \mathbf{X} + \epsilon) \\ &= \frac{1}{2} \log \frac{|\Sigma_{\mathbf{X}}| |\Sigma_{\mathbf{Y}} - \Sigma_{\mathbf{Y}\mathbf{X}} \Sigma_{\mathbf{X}}^{-1} \Sigma_{\mathbf{X}\mathbf{Y}}|}{|\Sigma_{\mathbf{X}+\epsilon}| |\Sigma_{\mathbf{Y}} - \Sigma_{\mathbf{Y}\mathbf{X}} \Sigma_{\mathbf{X}+\epsilon}^{-1} \Sigma_{\mathbf{X}\mathbf{Y}}|} \\ &= \frac{1}{2} \log \frac{1}{(1 + \sigma_{\epsilon}^2 \sum_{i=1}^k \frac{1}{\sigma_{X_i}^2}) (1 + \lambda \sum_{i=1}^k \frac{\text{cov}^2(X_i, Y_i)}{\sigma_{X_i}^2 (\sigma_{X_i}^2 \sigma_{Y_i}^2 - \text{cov}^2(X_i, Y_i))}} \end{aligned} \quad (11)$$

where  $\lambda = \frac{\sigma_{\epsilon}^2}{1 + \sum_{i=1}^k \frac{1}{\sigma_{X_i}^2}}$ ,  $\sigma_{\epsilon}^2$  is the variance of the Gaussian noise,  $\text{cov}(X_i, Y_i)$  is the covariance of

sample pair  $X_i, Y_i$ ,  $\sigma_{X_i}^2$  and  $\sigma_{Y_i}^2$  are the variance of data sample  $X_i$  and data label  $Y_i$ , respectively. The detailed derivations can be found in section 1.1.2 of the supplementary. Given a dataset, the variance of the Gaussian noise, and statistical properties of data samples and labels control the mutual information, we define the function:

$$\begin{aligned} f(\sigma_{\epsilon}^2) &= 1 - (1 + \sigma_{\epsilon}^2 \sum_{i=1}^k \frac{1}{\sigma_{X_i}^2}) (1 + \lambda \sum_{i=1}^k \frac{\text{cov}^2(X_i, Y_i)}{\sigma_{X_i}^2 (\sigma_{X_i}^2 \sigma_{Y_i}^2 - \text{cov}^2(X_i, Y_i))}) \\ &= -\sigma_{\epsilon}^2 \sum_{i=1}^k \frac{1}{\sigma_{X_i}^2} - \sigma_{\epsilon}^2 \sum_{i=1}^k \frac{1}{\sigma_{X_i}^2} \cdot \lambda \sum_{i=1}^k \frac{\text{cov}^2(X_i, Y_i)}{\sigma_{X_i}^2 (\sigma_{X_i}^2 \sigma_{Y_i}^2 - \text{cov}^2(X_i, Y_i))} - \lambda \sum_{i=1}^k \frac{\text{cov}^2(X_i, Y_i)}{\sigma_{X_i}^2 (\sigma_{X_i}^2 \sigma_{Y_i}^2 - \text{cov}^2(X_i, Y_i))} \end{aligned} \quad (12)$$

Since  $\epsilon^2 \geq 0$  and  $\lambda \geq 0$ ,  $\sigma_{X_i}^2 \sigma_{Y_i}^2 - \text{cov}^2(X_i, Y_i) = \sigma_{X_i}^2 \sigma_{Y_i}^2 (1 - \rho_{X_i Y_i}^2) \geq 0$ , where  $\rho_{X_i Y_i}$  is the correlation coefficient, the sign of  $f(\sigma_{\epsilon}^2)$  is negative. We can conclude that Gaussian noise injected into the latent space is harmful to the task. More details and the Gaussian noise added to the image level are provided in the supplementary.

**Linear Transform Noise** This type of noise is obtained by elementary transformation of the features matrix, i.e.,  $\epsilon = Q\mathbf{X}$ , where  $Q$  is a linear transformation matrix. We name the  $Q$  the quality matrix since it controls the property of linear transform noise and determines whether positive or harmful. In the linear transform noise injection in the latent space case, the complexity of the task is:

$$H(\mathcal{T}; \mathbf{X} + Q\mathbf{X}) = H(\mathbf{Y}; \mathbf{X} + Q\mathbf{X}) - H(\mathbf{X}) \quad (13)$$

The mutual information is then formulated as:

$$\begin{aligned}
MI(\mathcal{T}, Q\mathbf{X}) &= H(\mathbf{Y}; \mathbf{X}) - H(\mathbf{X}) - (H(\mathbf{Y}; \mathbf{X} + Q\mathbf{X}) - H(\mathbf{X})) \\
&= H(\mathbf{Y}; \mathbf{X}) - H(\mathbf{Y}; \mathbf{X} + Q\mathbf{X}) \\
&= \frac{1}{2} \log \frac{|\Sigma_{\mathbf{X}}| |\Sigma_{\mathbf{Y}} - \Sigma_{\mathbf{Y}\mathbf{X}} \Sigma_{\mathbf{X}}^{-1} \Sigma_{\mathbf{X}\mathbf{Y}}|}{|\Sigma_{(I+Q)\mathbf{X}}| |\Sigma_{\mathbf{Y}} - \Sigma_{\mathbf{Y}\mathbf{X}} \Sigma_{\mathbf{X}}^{-1} \Sigma_{\mathbf{X}\mathbf{Y}}|} \\
&= \frac{1}{2} \log \frac{1}{|I + Q|^2} \\
&= -\log |I + Q|
\end{aligned} \tag{14}$$

Since we want the mutual information to be greater than 0, we can formulate Equation 14 as an optimization problem:

$$\begin{aligned}
&\max_Q MI(\mathcal{T}, Q\mathbf{X}) \\
&s.t. \text{rank}(I + Q) = k \\
&\quad Q \sim I \\
&\quad [I + Q]_{ii} \geq [I + Q]_{ij}, i \neq j \\
&\quad \|[I + Q]_i\|_1 = 1
\end{aligned} \tag{15}$$

where  $\sim$  means the row equivalence. The key to determining whether the linear transform is positive noise or not lies in the matrix of  $Q$ . The most important step is to ensure that  $I + Q$  is reversible, which is  $|(I + Q)| \neq 0$ . The third constraint is to make the trained classifier get enough information about a specific image and correctly predict the corresponding label. For example, for an image  $X_1$  perturbed by another image  $X_2$ , the classifier obtained dominant information from  $X_1$  so that it can predict the label  $Y_1$ . However, if the perturbed image  $X_2$  is dominant, the classifier can hardly predict the correct label  $Y_1$  and is more likely to predict as  $Y_2$ . The fourth constraint is to maintain the norm of latent representations. More in-depth discussion and linear transform noise added to the image level are provided in the supplementary.

**Salt-and-pepper Noise** The salt-and-pepper noise is a common multiplicative noise for images. The image can exhibit unnatural changes, such as black pixels in bright areas or white pixels in dark areas, specifically as a result of the signal disruption caused by sudden strong interference or bit transmission errors. In the Salt-and-pepper noise case, the mutual information is:

$$\begin{aligned}
MI(\mathcal{T}, \epsilon) &= H(\mathbf{Y}; \mathbf{X}) - H(\mathbf{X}) - (H(\mathbf{Y}; \mathbf{X}\epsilon) - H(\mathbf{X})) \\
&= H(\mathbf{Y}; \mathbf{X}) - H(\mathbf{Y}; \mathbf{X}\epsilon) \\
&= -\sum_{\mathbf{X} \in \mathcal{X}} \sum_{\mathbf{Y} \in \mathcal{Y}} p(\mathbf{X}, \mathbf{Y}) \log p(\mathbf{X}, \mathbf{Y}) - \sum_{\mathbf{X} \in \mathcal{X}} \sum_{\mathbf{Y} \in \mathcal{Y}} \sum_{\epsilon \in \mathcal{E}} p(\mathbf{X}\epsilon, \mathbf{Y}) \log p(\mathbf{X}\epsilon, \mathbf{Y}) \\
&= \mathbb{E} \left[ \log \frac{1}{p(\mathbf{X}, \mathbf{Y})} \right] - \mathbb{E} \left[ \log \frac{1}{p(\mathbf{X}\epsilon, \mathbf{Y})} \right] \\
&= \mathbb{E} \left[ \log \frac{1}{p(\mathbf{X}, \mathbf{Y})} \right] - \mathbb{E} \left[ \log \frac{1}{p(\mathbf{X}, \mathbf{Y})} \right] - \mathbb{E} \left[ \log \frac{1}{p(\epsilon)} \right] \\
&= -H(\epsilon)
\end{aligned} \tag{16}$$

Obviously, the mutual information is smaller than 0, which indicates the complexity is increasing when injecting salt-and-pepper noise into the deep model. As can be foreseen, the salt-and-pepper noise is pure detrimental noise. More details and Salt-and-pepper added to the image level are in the supplementary.

## 4 Experiments

In this section, we conduct extensive experiments to explore the influence of various types of noises on deep learning models. We employ popular deep learning architectures, including both CNNs and ViTs, and show that the two kinds of deep models can benefit from the positive noise. We employ deep learning models of various scales, including ViT-Tiny (ViT-T), ViT-Small (ViT-S), ViT-Base (ViT-B), and ViT-Large (ViT-L) for Vision Transformers (ViTs), and ResNet-18, ResNet-34,

ResNet-50, and ResNet-101 for ResNet architecture. The details of deep models are presented in the supplementary. Without specific instructions, the noise is injected at the last layer of the deep models. Note that for ResNet models, the number of macro layers is 4, and for each macro layer, different scale ResNet models have different micro sublayers. For example, for ResNet-18, the number of macro layers is 4, and for each macro layer, the number of micro sublayers is 2. The noise is injected at the last micro sublayer of the last macro layer for ResNet models. More experimental settings for ResNet and ViT are detailed in the supplementary.

#### 4.1 Noise Setting

We utilize the standard normal distribution to generate Gaussian noise in our experiments, ensuring that the noise has zero mean and unit variance. Gaussian noise can be expressed as:

$$\epsilon \sim \mathcal{N}(0, 1) \quad (17)$$

For linear transform noise, we use a quality matrix of as:

$$Q = -\alpha I + \alpha f(I) \quad (18)$$

where  $I$  is the identity matrix,  $\alpha$  represents the linear transform strength and  $f$  is a row cyclic shift operation switching row to the next row, for example, in a  $3 \times 3$  matrix,  $f$  will move Row 1 to Row 2, Row 2 to Row 3, and Row 3 to Row 1. For salt-and-pepper noise, we also use the parameter  $\alpha$  to control the probability of the emergence of salt-and-pepper noise, which can be formulated as:

$$\begin{cases} \max(X) & \text{if } p < \alpha/2 \\ \min(X) & \text{if } p > 1 - \alpha/2 \end{cases} \quad (19)$$

where  $p$  is a probability generated by a random seed,  $\alpha \in [0, 1)$ , and  $X$  is the representation of an image.

#### 4.2 Image Classification Results

We implement extensive experiments on large-scale datasets such as ImageNet [13] and small-scale datasets such as TinyImageNet [26] using ResNets and ViTs.

##### 4.2.1 CNN Family

The results of ResNets with different noises on ImageNet are in Table 1. As shown in the table, with the design of linear transform noise to be positive noise (PN), ResNet improves the classification accuracy by a large margin. While the salt-and-pepper, which is theoretically harmful noise (HN), degrades the models. Note we did not utilize data augmentation techniques for ResNet experiments except for normalization. The significant results show that positive noise can effectively improve classification accuracy by reducing task complexity.

##### 4.2.2 ViT Family

The results of ViT with different noises on ImageNet are in Table 2. Since the ViT-L is overfitting on the ImageNet [15] [53], the positive noise did not work well on the ViT-L. As shown in the table, the existence of positive noise improves the classification accuracy of ViT by a large margin compared to vanilla ViT. The comparisons with previously published works, such as DeiT [58], SwinTransformer [32], DaViT [14], and MaxViT [59], are shown in Table 3, and our positive noise-empowered ViT achieved the new state-of-the-art result. Note that the JFT-300M and JFT-4B datasets are private and not publicly available [55], and we believe that ViT large and above will benefit from positive noise significantly if trained on larger JFT-300M or JFT-4B, which is theoretically supported in section 4.4.

#### 4.3 Ablation Study

We also proactively inject noise into variants of ViT, such as DeiT [58], Swin Transformer [32], BEiT [3], and ConViT [11], and the results show that positive noise could benefit various variants of ViT by improving classification accuracy significantly. The results of injecting noise to variants

Table 1: ResNet with different kinds of noise on ImageNet. Vanilla means the vanilla model without noise. Accuracy is shown in percentage. Gaussian noise used here is subjected to standard normal distribution. Linear transform noise used in this table is designed to be positive noise. The difference is shown in the bracket.

Model	ResNet-18	ResNet-34	ResNet-50	ResNet-101
Vanilla	63.90 (+0.00)	66.80 (+0.00)	70.00 (+0.00)	70.66 (+0.00)
+ Gaussian Noise	62.35 (-1.55)	65.40 (-1.40)	69.62 (-0.33)	70.10 (-0.56)
+ Linear Transform Noise	<b>79.62 (+15.72)</b>	<b>80.05 (+13.25)</b>	<b>81.32 (+11.32)</b>	<b>81.91 (+11.25)</b>
+ Salt-and-pepper Noise	55.45 (-8.45)	63.36 (-3.44)	45.89 (-24.11)	52.96 (-17.70)

Table 2: ViT with different kinds of noise on ImageNet. Vanilla means the vanilla model without injecting noise. Accuracy is shown in percentage. Gaussian noise used here is subjected to standard normal distribution. Linear transform noise used in this table is designed to be positive noise. The difference is shown in the bracket. Note **ViT-L is overfitting on ImageNet** [15] [53].

Model	ViT-T	ViT-S	ViT-B	ViT-L
Vanilla	79.34 (+0.00)	81.88 (+0.00)	84.33 (+0.00)	88.64 (+0.00)
+ Gaussian Noise	79.10 (-0.24)	81.80 (-0.08)	83.41 (-0.92)	85.92 (-2.72)
+ Linear Transform Noise	<b>80.69 (+1.35)</b>	<b>87.27 (+5.39)</b>	<b>89.99 (+5.66)</b>	<b>88.72 (+0.08)</b>
+ Salt-and-pepper Noise	78.64 (-0.70)	81.75 (-0.13)	82.40 (-1.93)	85.15 (-3.49)

of ViT are reported in the supplementary. We also did ablation studies on the strength of linear transform noise and the injected layer. The results are shown in Fig. 2. We can observe that the deeper layer the positive noise injects, the better prediction performance the model can obtain. There are reasons behind this phenomenon. First, the latent features of input in the deeper layer have better representations than those in shallow layers; second, injection to shallow layers obtain less mutual information gain because of trendy replacing Equation 9 with Equation 8. More results on the small dataset TinyImageNet can be found in the supplementary.

Additionally, we tested the positive linear transformation noise on another popular dataset, the ImageNet V2. The corresponding results are reported in Table 4.

#### 4.4 Optimal Quality Matrix

As shown in Equation 15, it is interesting to learn about the optimal quality matrix of  $Q$  that maximizes the mutual information while satisfying the constraints. This equals minimizing the determinant of the matrix sum of  $I$  and  $Q$ . Here, we directly give out the optimal quality matrix of  $Q$  as:

$$Q_{optimal} = \text{diag} \left( \frac{1}{k+1} - 1, \dots, \frac{1}{k+1} - 1 \right) + \frac{1}{k+1} \mathbf{1}_{k \times k} \quad (20)$$

where  $k$  is the number of data samples. And the corresponding upper boundary of the mutual information as:

$$MI(\mathcal{T}, Q_{optimal} \mathbf{X}) = (k-1) \log(k+1) \quad (21)$$

The details are provided in the supplementary. We find that the upper boundary of the mutual information of injecting positive noise is determined by the number of data samples, i.e., the scale of

Table 3: Comparison between Positive Noise Empowered ViT with other ViT variants. Top 1 Accuracy is shown in percentage. Here PN is the positive noise, i.e., linear transform noise.

Model	Top1 Acc.	Params.	Image Res.	Pretrained Dataset
ViT-B [15]	84.33	86M	224 × 224	ImageNet 21k
DeiT-B [58]	85.70	86M	224 × 224	ImageNet 21k
SwinTransformer-B [32]	86.40	88M	384 × 384	ImageNet 21k
DaViT-B [14]	86.90	88M	384 × 384	ImageNet 21k
MaxViT-B [59]	88.82	119M	512 × 512	JFT-300M (Private)
ViT-22B [12]	89.51	21743M	224 × 224	JFT-4B (Private)
ViT-B+PN	<b>89.99</b>	86M	224 × 224	ImageNet 21k
ViT-B+PN	<b>91.37</b>	86M	384 × 384	ImageNet 21k

Table 4: Top 1 accuracy on ImageNet V2 with positive linear transform noise.

Model	Top1 Acc.	Params.	Image Res.	Pretrained Dataset
ViT-B+PN	<b>82.20</b>	86M	224 × 224	ImageNet 21k
ViT-B+PN	<b>84.80</b>	86M	384 × 384	ImageNet 21k

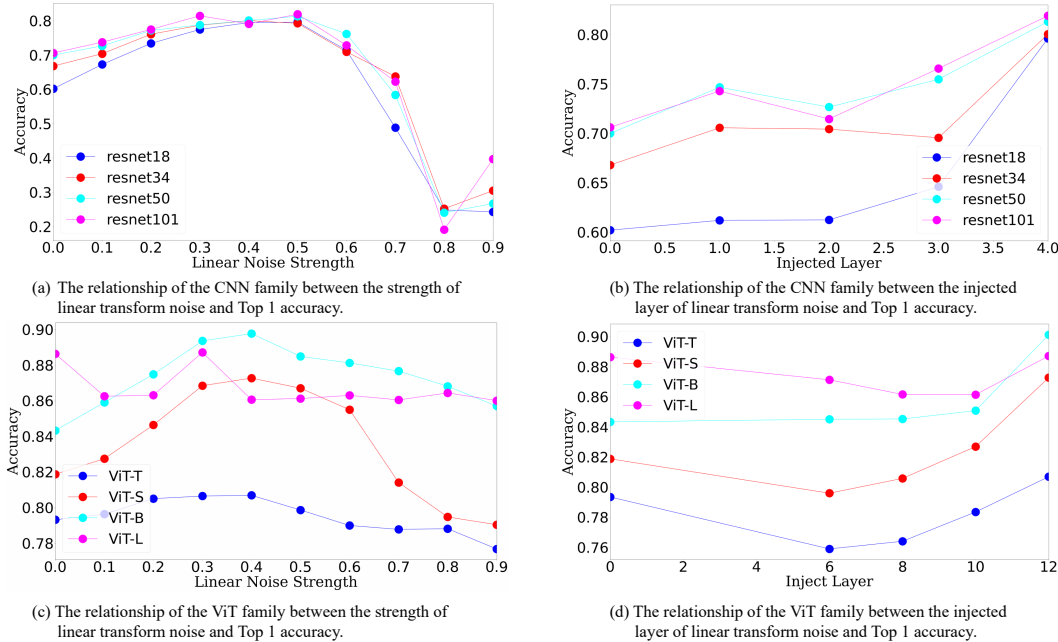


Figure 2: The relationship between the linear transform noise strength and the top 1 accuracy, and between the injected layer and top 1 accuracy. Parts (a) and (b) are the results of the CNN family, while parts (c) and (d) are the results of the ViT family. For parts (a) and (c) the linear transform noise is injected at the last layer. For parts (b) and (d), the influence of positive noise on different layers is shown. Layers 6, 8, 10, and 12 in the ViT family are chosen for the ablation study.

the dataset. Therefore, the larger the dataset, the better effect of injecting positive noise into deep models. With the optimal quality matrix and the top 1 accuracy of ViT-B on ImageNet can be further improved to 95%, which is shown in Table 5.

#### 4.5 Domain Adaption Results

Unsupervised domain adaptation (UDA) aims to learn transferable knowledge across the source and target domains with different distributions [41] [62]. Recently, transformer-based methods achieved SOTA results on UDA, therefore, we evaluate the ViT-B with the positive noise on widely used UDA benchmarks. Here the positive noise is the linear transform noise identical to that used in the classification task. The positive noise is injected into the last layer of the model, the same as the classification task. The datasets include **Office Home** [61] and **VisDA2017** [42]. Detailed datasets introduction and experiments training settings are in the supplementary. The objective function is borrowed from TVT [66], which is the first work that adopts Transformer-based architecture for UDA. The results are shown in Table 6 and 7. The ViT-B with positive noise achieves better

Table 5: Top 1 accuracy on ImageNet with the optimal quality matrix of linear transform noise.

Model	Top1 Acc.	Params.	Image Res.	Pretrained Dataset
ViT-B+Optimal Q	<b>93.87</b>	86M	224 × 224	ImageNet 21k
ViT-B+Optimal Q	<b>95.12</b>	86M	384 × 384	ImageNet 21k

Table 6: Comparison with various ViT-based methods on **Office-Home**.

Method	Ar2C1	Ar2Pr	Ar2Re	Cl2Ar	Cl2Pr	Cl2Re	Pr2Ar	Pr2Cl	Pr2Re	Re2Ar	Re2Cl	Re2Pr	Avg.
ViT-B [15]	54.7	83.0	87.2	77.3	83.4	85.6	74.4	50.9	87.2	79.6	54.8	88.8	75.5
TVT-B [66]	74.9	86.8	89.5	82.8	88.0	88.3	79.8	71.9	90.1	85.5	74.6	90.6	83.6
CDTrans-B [65]	68.8	85.0	86.9	81.5	87.1	87.3	79.6	63.3	88.2	82.0	66.0	90.6	80.5
SSRT-B [56]	75.2	89.0	91.1	85.1	88.3	90.0	85.0	74.2	91.3	85.7	78.6	91.8	85.4
TVT-B+PN	<b>78.3</b>	<b>90.6</b>	<b>91.9</b>	<b>87.8</b>	<b>92.1</b>	<b>91.9</b>	<b>85.8</b>	<b>78.7</b>	<b>93.0</b>	<b>88.6</b>	<b>80.6</b>	<b>93.5</b>	<b>87.7</b>

Table 7: Comparison with various ViT-based methods on **Visda2017**.

Method	plane	bcycl	bus	car	horse	knife	mcycl	person	plant	sktbrd	train	truck	Avg.
ViT-B [15]	97.7	48.1	86.6	61.6	78.1	63.4	94.7	10.3	87.7	47.7	94.4	35.5	67.1
TVT-B [66]	92.9	85.6	77.5	60.5	93.6	98.2	89.4	76.4	93.6	92.0	91.7	55.7	83.9
CDTrans-B [65]	97.1	90.5	82.4	77.5	96.6	96.1	93.6	<b>88.6</b>	<b>97.9</b>	86.9	90.3	62.8	88.4
SSRT-B [56]	<b>98.9</b>	87.6	<b>89.1</b>	<b>84.8</b>	98.3	<b>98.7</b>	<b>96.3</b>	81.1	94.9	97.9	94.5	43.1	88.8
TVT-B+PN	98.8	<b>95.5</b>	84.8	73.7	<b>98.5</b>	97.2	95.1	76.5	95.9	<b>98.4</b>	<b>98.3</b>	<b>67.2</b>	<b>90.0</b>

performance than the existing works. These results show that positive noise can improve model generality, therefore, benefit deep models in domain adaptation tasks.

## 5 Conclusion

This study delves into the influence of entropy change on learning systems, achieved by proactively introducing various types of noise into deep models. Our work conducts a comprehensive investigation into the impact of common noise types, such as Gaussian noise, linear transform noise, and salt-and-pepper noise, on deep learning models. Notably, we demonstrate that, under specific conditions, linear transform noise can positively affect deep models. The experimental results show that injecting positive noise into the latent space significantly enhances the prediction performance of deep models in image classification tasks, leading to new state-of-the-art results on ImageNet. These findings hold broad implications for future research and the potential development of more accurate models for improved real-world applications. Furthermore, the proposed theory is versatile, and we look forward to exploring the application of positive noise in various deep learning tasks within computer vision and natural language processing.

## A The Influence of Noise on Task Entropy

This section shows the detailed derivations of the conclusion of three kinds of noise on the variations of task entropy. As stated in this paper, the noises can be categorized into additive and multiplicative noise. We list the original task entropy and rewrite task entropy with additive and multiplicative noise, separately.

The original task entropy is formulated as [29]:

$$H(\mathcal{T}; \mathbf{X}) = - \sum_{\mathbf{Y} \in \mathcal{Y}} p(\mathbf{Y}|\mathbf{X}) \log p(\mathbf{Y}|\mathbf{X}) \quad (22)$$

The images  $\mathbf{X}$  in the dataset are supposed to be independent of each other, as are the labels  $\mathbf{Y}$ . However,  $\mathbf{X}$  and  $\mathbf{Y}$  are not independent because of the correlation between a data sample  $X$  and its corresponding label  $Y$ , the conditional distribution of  $\mathbf{Y}$  given  $\mathbf{X}$  will depend on the joint distribution of  $\mathbf{X}$  and  $\mathbf{Y}$ . Without knowing the joint distribution of  $\mathbf{X}$  and  $\mathbf{Y}$ , we can not determine the conditional distribution of  $\mathbf{Y}$  and  $\mathbf{X}$ . Here, we make some slacks for the distribution of  $\mathbf{X}$  and  $\mathbf{Y}$ . We can transform the unknown distributions of  $\mathbf{X}$  and  $\mathbf{Y}$  to approximately conform to normality by utilizing some techniques, such as Box-Cox transformation, log transform, etc [5] [17]. After approximate transformation, the distribution of  $\mathbf{X}$  and  $\mathbf{Y}$  can be expressed as:

$$\mathbf{X} \sim \mathcal{N}(\boldsymbol{\mu}_X, \boldsymbol{\Sigma}_X), \mathbf{Y} \sim \mathcal{N}(\boldsymbol{\mu}_Y, \boldsymbol{\Sigma}_Y) \quad (23)$$

where

$$\begin{aligned} \boldsymbol{\mu}_X &= \mathbb{E}[\mathbf{X}] = (\mathbb{E}[X_1], \mathbb{E}[X_2], \dots, \mathbb{E}[X_k])^T \\ \boldsymbol{\mu}_Y &= \mathbb{E}[\mathbf{Y}] = (\mathbb{E}[Y_1], \mathbb{E}[Y_2], \dots, \mathbb{E}[Y_k])^T \\ \boldsymbol{\Sigma}_X &= \mathbb{E}[(\mathbf{X} - \boldsymbol{\mu}_X)(\mathbf{X} - \boldsymbol{\mu}_X)^T] \\ \boldsymbol{\Sigma}_Y &= \mathbb{E}[(\mathbf{Y} - \boldsymbol{\mu}_Y)(\mathbf{Y} - \boldsymbol{\mu}_Y)^T] \end{aligned} \quad (24)$$

$k$  is the number of samples in the dataset, and  $T$  represents the transpose of the matrix.

After transformation, the  $\mathbf{X}$  and  $\mathbf{Y}$  are subjected to multivariate normal distribution. Then the conditional distribution of  $\mathbf{Y}$  given  $\mathbf{X}$  is also normally distributed [37] [23], which can be formulated as:

$$\mathbf{Y}|\mathbf{X} \sim \mathcal{N}(\mathbb{E}(\mathbf{Y}|\mathbf{X} = \mathbf{x}), \text{var}(\mathbf{Y}|\mathbf{X} = \mathbf{x})) \quad (25)$$

where  $\mathbb{E}(\mathbf{Y}|\mathbf{X} = \mathbf{x})$  is the mean of the label set  $\mathbf{Y}$  given a sample  $\mathbf{X} = \mathbf{x}$  from the dataset, and  $\text{var}(\mathbf{Y}|\mathbf{X} = \mathbf{x})$  is the variance of  $\mathbf{Y}$  given a sample from the dataset. The conditional mean  $\mathbb{E}[(\mathbf{Y}|\mathbf{X} = \mathbf{x})]$  and conditional variance  $\text{var}(\mathbf{Y}|\mathbf{X} = \mathbf{x})$  can be calculated as:

$$\boldsymbol{\mu}_{\mathbf{Y}|\mathbf{X}=\mathbf{x}} = \mathbb{E}[(\mathbf{Y}|\mathbf{X} = \mathbf{x})] = \boldsymbol{\mu}_Y + \boldsymbol{\Sigma}_{\mathbf{Y}\mathbf{X}}\boldsymbol{\Sigma}_X^{-1}(\mathbf{x} - \boldsymbol{\mu}_X) \quad (26)$$

$$\boldsymbol{\Sigma}_{\mathbf{Y}|\mathbf{X}=\mathbf{x}} = \text{var}(\mathbf{Y}|\mathbf{X} = \mathbf{x}) = \boldsymbol{\Sigma}_Y - \boldsymbol{\Sigma}_{\mathbf{Y}\mathbf{X}}\boldsymbol{\Sigma}_X^{-1}\boldsymbol{\Sigma}_{\mathbf{X}\mathbf{Y}} \quad (27)$$

where  $\boldsymbol{\Sigma}_{\mathbf{Y}\mathbf{X}}$  and  $\boldsymbol{\Sigma}_{\mathbf{X}\mathbf{Y}}$  are the cross-covariance matrices between  $\mathbf{Y}$  and  $\mathbf{X}$ , and between  $\mathbf{X}$  and  $\mathbf{Y}$ , respectively, and  $\boldsymbol{\Sigma}_X^{-1}$  denotes the inverse of the covariance matrix of  $\mathbf{X}$ .

Now, let  $\mathbf{Z} = \mathbf{Y}|\mathbf{X}$ , we shall obtain the task entropy:

$$\begin{aligned} H(\mathcal{T}; \mathbf{X}) &= - \sum_{\mathbf{Y} \in \mathcal{Y}} p(\mathbf{Y}|\mathbf{X}) \log p(\mathbf{Y}|\mathbf{X}) \\ &= - \mathbb{E}[\log p(\mathbf{Y}|\mathbf{X})] \\ &= - \mathbb{E}[\log[(2\pi)^{-k/2} |\boldsymbol{\Sigma}_Z|^{-1/2} \exp(-\frac{1}{2}(\mathbf{Z} - \boldsymbol{\mu}_Z)^T \boldsymbol{\Sigma}_Z^{-1}(\mathbf{Z} - \boldsymbol{\mu}_Z))]] \quad (28) \\ &= \frac{k}{2} \log(2\pi) + \frac{1}{2} \log |\boldsymbol{\Sigma}_Z| + \frac{1}{2} \mathbb{E}[(\mathbf{Z} - \boldsymbol{\mu}_Z)^T \boldsymbol{\Sigma}_Z^{-1}(\mathbf{Z} - \boldsymbol{\mu}_Z)] \\ &= \frac{k}{2} (1 + \log(2\pi)) + \frac{1}{2} \log |\boldsymbol{\Sigma}_Z| \end{aligned}$$

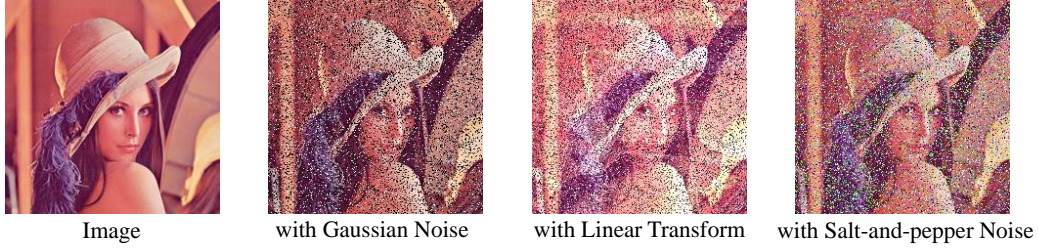


Figure 3: The influence of noise on the image. From left to right are the original image, the image with Gaussian noise, overlapping with its own linear transform, and with salt-and-pepper noise, separately.

where

$$\begin{aligned}
\mathbb{E}[(\mathbf{Z} - \boldsymbol{\mu}_{\mathbf{Z}})^T \Sigma_{\mathbf{Z}}^{-1} (\mathbf{Z} - \boldsymbol{\mu}_{\mathbf{Z}})] &= \mathbb{E}[\text{tr}((\mathbf{Z} - \boldsymbol{\mu}_{\mathbf{Z}})^T \Sigma_{\mathbf{Z}}^{-1} (\mathbf{Z} - \boldsymbol{\mu}_{\mathbf{Z}}))] \\
&= \mathbb{E}[\text{tr}(\Sigma_{\mathbf{Z}}^{-1} (\mathbf{Z} - \boldsymbol{\mu}_{\mathbf{Z}}) (\mathbf{Z} - \boldsymbol{\mu}_{\mathbf{Z}})^T)] \\
&= \text{tr}(\Sigma_{\mathbf{Z}}^{-1} (\mathbf{Z} - \boldsymbol{\mu}_{\mathbf{Z}}) (\mathbf{Z} - \boldsymbol{\mu}_{\mathbf{Z}})^T) \\
&= \text{tr}(\Sigma_{\mathbf{Z}}^{-1} \Sigma_{\mathbf{Z}}) \\
&= \text{tr}(\mathbf{I}_k) \\
&= k
\end{aligned} \tag{29}$$

Therefore, for a specific dataset, we can find that the task entropy is only related to the variance of the  $\mathbf{Z}$ .

However, as we proactively inject additional information into the latent space, the task entropy changes and is defined as :

$$\begin{cases} H(\mathcal{T}; \mathbf{X} + \boldsymbol{\epsilon}) := H(\mathbf{Y}; \mathbf{X} + \boldsymbol{\epsilon}) - H(\mathbf{X}) & \boldsymbol{\epsilon} \text{ is additive noise} \\ H(\mathcal{T}; \mathbf{X}\boldsymbol{\epsilon}) := H(\mathbf{Y}; \mathbf{X}\boldsymbol{\epsilon}) - H(\mathbf{X}) & \boldsymbol{\epsilon} \text{ is multiplicative noise} \end{cases} \tag{30}$$

Eq. 30 differs from the conventional definition of conditional entropy, as our method injects the noise into the latent representations instead of the original images. If adding noise to the original images, then we have the classic definition:

$$\begin{cases} H(\mathcal{T}; \mathbf{X} + \boldsymbol{\epsilon}) = H(\mathbf{Y}; \mathbf{X} + \boldsymbol{\epsilon}) - H(\mathbf{X} + \boldsymbol{\epsilon}) & \boldsymbol{\epsilon} \text{ is additive noise} \\ H(\mathcal{T}; \mathbf{X}\boldsymbol{\epsilon}) = H(\mathbf{Y}; \mathbf{X}\boldsymbol{\epsilon}) - H(\mathbf{X}\boldsymbol{\epsilon}) & \boldsymbol{\epsilon} \text{ is multiplicative noise} \end{cases} \tag{31}$$

Examples of the influence of various noises on the image level are provided in Fig. 3.

### A.1 Influence of Gaussian Noise on Task Entropy

Gaussian is one of the most common noises in image processing, and it is an additive noise. The Gaussian noise  $\boldsymbol{\epsilon}$  is subjected to the normal distribution of  $\boldsymbol{\epsilon} \sim \mathcal{N}(\mu_{\boldsymbol{\epsilon}}, \sigma_{\boldsymbol{\epsilon}})$  and is independent of  $\mathbf{X}$  and  $\mathbf{Y}$ . As we stated that the noise can be added to the original images or injected into the latent space, therefore, we discuss the conditions separately.

#### A.1.1 Add Gaussian Noise to Original Images

The task entropy with Gaussian noise is rewritten as:

$$H(\mathcal{T}; \mathbf{X} + \boldsymbol{\epsilon}) = - \sum_{\mathbf{Y} \in \mathcal{Y}} p(\mathbf{Y} | \mathbf{X} + \boldsymbol{\epsilon}) \log p(\mathbf{Y} | \mathbf{X} + \boldsymbol{\epsilon}) \tag{32}$$

Follow the derivations of the task entropy, we can calculate the task entropy with additive Gaussian noise as:

$$\begin{aligned}
H(\mathcal{T}; \mathbf{X} + \boldsymbol{\epsilon}) &= - \sum_{\mathbf{Y} \in \mathcal{Y}} p(\mathbf{Y} | \mathbf{X} + \boldsymbol{\epsilon}) \log p(\mathbf{Y} | \mathbf{X} + \boldsymbol{\epsilon}) \\
&= - \mathbb{E}[\log p(\mathbf{Y} | \mathbf{X} + \boldsymbol{\epsilon})] \\
&= \frac{k}{2} (1 + \log(2\pi)) + \frac{1}{2} \log |\boldsymbol{\Sigma}_{\mathbf{Y} | \mathbf{X} + \boldsymbol{\epsilon}}|
\end{aligned} \tag{33}$$

where  $\Sigma_{Y|X+\epsilon} = \Sigma_Y - \Sigma_{Y(X+\epsilon)}\Sigma_{X+\epsilon}^{-1}\Sigma_{(X+\epsilon)Y}$ . Since the Gaussian noise is independent of  $X$  and  $Y$ , we have  $\Sigma_{Y(X+\epsilon)} = \Sigma_{(X+\epsilon)Y} = \Sigma_{YX}$ . The corresponding proof is:

$$\begin{aligned}
\Sigma_{(X+\epsilon)Y} &= \mathbb{E}[(X + \epsilon) - \mu_{X+\epsilon}] \mathbb{E}[Y - \mu_Y] \\
&= \mathbb{E}[(X + \epsilon)Y] - \mu_Y \mathbb{E}[(X + \epsilon)] - \mu_{X+\epsilon} \mathbb{E}[Y] + \mu_Y \mu_{X+\epsilon} \\
&= \mathbb{E}[(X + \epsilon)Y] - \mu_Y \mathbb{E}[(X + \epsilon)] \\
&= \mathbb{E}[XY] + \mathbb{E}[\epsilon Y] - \mu_Y \mu_X - \mu_Y \mu_\epsilon \\
&= \mathbb{E}[XY] - \mu_Y \mu_X \\
&= \Sigma_{XY}
\end{aligned} \tag{34}$$

Thus, the variation of task entropy adding Gaussian noise can be formulated as:

$$\begin{aligned}
MI(\mathcal{T}, \epsilon) &= H(\mathcal{T}; X) - H(\mathcal{T}; X + \epsilon) \\
&= \frac{1}{2} \log |\Sigma_{Y|X}| - \frac{1}{2} \log |\Sigma_{Y|X+\epsilon}| \\
&= \frac{1}{2} \log \frac{|\Sigma_{Y|X}|}{|\Sigma_{Y|X+\epsilon}|} \\
&= \frac{1}{2} \log \frac{|\Sigma_Y - \Sigma_{YX}\Sigma_X^{-1}\Sigma_{XY}|}{|\Sigma_Y - \Sigma_{Y(X+\epsilon)}\Sigma_{X+\epsilon}^{-1}\Sigma_{(X+\epsilon)Y}|} \\
&= \frac{1}{2} \log \frac{|\Sigma_Y - \Sigma_{YX}\Sigma_X^{-1}\Sigma_{XY}|}{|\Sigma_Y - \Sigma_{YX}\Sigma_{X+\epsilon}^{-1}\Sigma_{XY}|}
\end{aligned} \tag{35}$$

Obviously,

$$\begin{cases} MI(\mathcal{T}, \epsilon) > 0 & \text{if } \frac{|\Sigma_{Y|X}|}{|\Sigma_{Y|X+\epsilon}|} > 1 \\ MI(\mathcal{T}, \epsilon) \leq 0 & \text{if } \frac{|\Sigma_{Y|X}|}{|\Sigma_{Y|X+\epsilon}|} \leq 1 \end{cases} \tag{36}$$

To find the relationship between  $|\Sigma_{Y|X+\epsilon}|$  and  $|\Sigma_{Y|X}|$ , we need to determine the subterms in each of them. As we mentioned in the previous section, the data samples are independent of each other, and so are the labels.

$$\begin{aligned}
\Sigma_Y &= \mathbb{E}[(Y - \mu_Y)(Y - \mu_Y)^T] \\
&= \mathbb{E}[YY^T] - \mu_Y \mu_Y^T \\
&= \text{diag}(\sigma_{Y_1}^2, \dots, \sigma_{Y_k}^2)
\end{aligned} \tag{37}$$

where

$$\begin{cases} \mathbb{E}[Y_i Y_j] - \mu_{Y_i} \mu_{Y_j} = 0, & i \neq j \\ \mathbb{E}[Y_i Y_j] - \mu_{Y_i} \mu_{Y_j} = \sigma_{Y_i}^2, & i = j \end{cases} \tag{38}$$

The same procedure can be applied to  $\Sigma_{Y(X+\epsilon)}$  and  $\Sigma_{X+\epsilon}$ . Therefore, We can obtain that  $\Sigma_Y = \text{diag}(\sigma_{Y_1}^2, \dots, \sigma_{Y_k}^2)$ ,  $\Sigma_{Y(X+\epsilon)} = \text{diag}(\text{cov}(Y_1, X_1 + \epsilon), \dots, \text{cov}(Y_k, X_k + \epsilon))$ , and  $\Sigma_{X+\epsilon}$  is:

$$\begin{aligned}
\Sigma_{X+\epsilon} &= \begin{bmatrix} \sigma_{X_1}^2 + \sigma_\epsilon^2 & \sigma_\epsilon^2 & \dots & \sigma_\epsilon^2 & \sigma_\epsilon^2 \\ \sigma_\epsilon^2 & \sigma_{X_2}^2 + \sigma_\epsilon^2 & \dots & \sigma_\epsilon^2 & \sigma_\epsilon^2 \\ \vdots & \vdots & \dots & \vdots & \vdots \\ \sigma_\epsilon^2 & \sigma_\epsilon^2 & \dots & \sigma_{X_{k-1}}^2 + \sigma_\epsilon^2 & \sigma_\epsilon^2 \\ \sigma_\epsilon^2 & \sigma_\epsilon^2 & \dots & \sigma_\epsilon^2 & \sigma_{X_k}^2 + \sigma_\epsilon^2 \end{bmatrix} \\
&= \text{diag}(\sigma_{X_1}^2, \dots, \sigma_{X_k}^2) \mathbf{I}_k + \sigma_\epsilon^2 \mathbf{1}_k
\end{aligned} \tag{39}$$

where  $\mathbf{I}_k$  is a  $k \times k$  identity matrix and  $\mathbf{1}_k$  is a all ones  $k \times k$  matrix. We use  $\mathbf{U}$  to represent  $\text{diag}(\sigma_{X_1}^2, \dots, \sigma_{X_k}^2) \mathbf{I}_k$ , and  $\mathbf{u}$  to represent a all ones vector  $[1, \dots, 1]^T$ . Thanks to the Sherman–Morrison Formula [50] and Woodbury Formula [63], we can obtain the inverse of  $\Sigma_{X+\epsilon}$

as:

$$\begin{aligned}
\Sigma_{\mathbf{X}+\epsilon}^{-1} &= (\mathbf{U} + \sigma_\epsilon^2 \mathbf{u}\mathbf{u}^T)^{-1} \\
&= \mathbf{U}^{-1} - \frac{\sigma_\epsilon^2}{1 + \sigma_\epsilon^2 \mathbf{u}^T \mathbf{U}^{-1} \mathbf{u}} \mathbf{U}^{-1} \mathbf{u}\mathbf{u}^T \mathbf{U}^{-1} \\
&= \mathbf{U}^{-1} - \frac{\sigma_\epsilon^2}{1 + \sum_{i=1}^k \frac{1}{\sigma_{X_i}^2}} \mathbf{U}^{-1} \mathbf{1}_k \mathbf{U}^{-1} \\
&= \lambda \begin{bmatrix} \frac{1}{\lambda \sigma_{X_1}^2} - \frac{1}{\sigma_{X_1}^4} & -\frac{1}{\sigma_{X_1}^2 \sigma_{X_2}^2} & \cdots & -\frac{1}{\sigma_{X_1}^2 \sigma_{X_{k-1}}^2} & -\frac{1}{\sigma_{X_1}^2 \sigma_{X_k}^2} \\ -\frac{1}{\sigma_{X_2}^2 \sigma_{X_1}^2} & \frac{1}{\lambda \sigma_{X_2}^2} - \frac{1}{\sigma_{X_2}^4} & \cdots & -\frac{1}{\sigma_{X_2}^2 \sigma_{X_{k-1}}^2} & -\frac{1}{\sigma_{X_2}^2 \sigma_{X_k}^2} \\ \vdots & \vdots & \ddots & \vdots & \vdots \\ -\frac{1}{\sigma_{X_{k-1}}^2 \sigma_{X_1}^2} & -\frac{1}{\sigma_{X_{k-1}}^2 \sigma_{X_2}^2} & \cdots & \frac{1}{\lambda \sigma_{X_{k-1}}^2} - \frac{1}{\sigma_{X_{k-1}}^4} & -\frac{1}{\sigma_{X_{k-1}}^2 \sigma_{X_k}^2} \\ -\frac{1}{\sigma_{X_k}^2 \sigma_{X_1}^2} & -\frac{1}{\sigma_{X_k}^2 \sigma_{X_2}^2} & \cdots & -\frac{1}{\sigma_{X_k}^2 \sigma_{X_{k-1}}^2} & \frac{1}{\lambda \sigma_{X_k}^2} - \frac{1}{\sigma_{X_k}^4} \end{bmatrix} \quad (40)
\end{aligned}$$

where  $\mathbf{U}^{-1} = \text{diag}((\sigma_{X_1}^2)^{-1}, \dots, (\sigma_{X_k}^2)^{-1})$  and  $\lambda = \frac{\sigma_\epsilon^2}{1 + \sum_{i=1}^k \frac{1}{\sigma_{X_i}^2}}$ .

Therefore, substitute Equation 40 into  $|\Sigma_{\mathbf{Y}} - \Sigma_{\mathbf{Y}(\mathbf{X}+\epsilon)} \Sigma_{\mathbf{X}+\epsilon}^{-1} \Sigma_{(\mathbf{X}+\epsilon)\mathbf{Y}}|$ , we can obtain:

$$\begin{aligned}
& |\Sigma_{\mathbf{Y}} - \Sigma_{\mathbf{Y}(\mathbf{X}+\epsilon)} \Sigma_{\mathbf{X}+\epsilon}^{-1} \Sigma_{(\mathbf{X}+\epsilon)\mathbf{Y}}| \\
&= \left| \begin{bmatrix} \sigma_{Y_1}^2 & \cdots & 0 \\ \vdots & \ddots & \vdots \\ 0 & \cdots & \sigma_{Y_k}^2 \end{bmatrix} - \begin{bmatrix} \text{cov}(Y_1, X_1 + \epsilon) & \cdots & 0 \\ \vdots & \ddots & \vdots \\ 0 & \cdots & \text{cov}(Y_k, X_k + \epsilon) \end{bmatrix} \Sigma_{\mathbf{X}+\epsilon}^{-1} \begin{bmatrix} \text{cov}(Y_1, X_1 + \epsilon) & \cdots & 0 \\ \vdots & \ddots & \vdots \\ 0 & \cdots & \text{cov}(Y_k, X_k + \epsilon) \end{bmatrix} \right| \\
&= \left| \begin{bmatrix} \sigma_{Y_1}^2 - \text{cov}^2(Y_1, X_1 + \epsilon) \left( \frac{1}{\sigma_{X_1}^2} - \frac{\lambda}{\sigma_{X_1}^4} \right) & \cdots & \text{cov}(Y_1, X_1 + \epsilon) \text{cov}(Y_k, X_k + \epsilon) \frac{\lambda}{\sigma_{X_1}^2 \sigma_{X_k}^2} \\ \vdots & \ddots & \vdots \\ \text{cov}(Y_k, X_k + \epsilon) \text{cov}(Y_1, X_1 + \epsilon) \frac{\lambda}{\sigma_{X_k}^2 \sigma_{X_1}^2} & \cdots & \sigma_{Y_k}^2 - \text{cov}^2(Y_k, X_k + \epsilon) \left( \frac{1}{\sigma_{X_k}^2} - \frac{\lambda}{\sigma_{X_k}^4} \right) \end{bmatrix} \right| \\
&= \left| \begin{bmatrix} \sigma_{Y_1}^2 - \frac{1}{\sigma_{X_1}^2} \text{cov}^2(Y_1, X_1) & \cdots & \frac{1}{\sigma_{X_1}^2} \text{cov}(Y_1, X_1) \text{cov}(Y_k, X_k) \\ \vdots & \ddots & \vdots \\ \frac{1}{\sigma_{X_k}^2} \text{cov}(Y_k, X_k) \text{cov}(Y_1, X_1) & \cdots & \sigma_{Y_k}^2 - \frac{1}{\sigma_{X_k}^2} \text{cov}^2(Y_k, X_k) \end{bmatrix} + \lambda \begin{bmatrix} \frac{1}{\sigma_{X_1}^2} \text{cov}^2(Y_1, X_1) & \cdots & \frac{1}{\sigma_{X_1}^2 \sigma_{X_k}^2} \text{cov}(Y_1, X_1) \text{cov}(Y_k, X_k) \\ \vdots & \ddots & \vdots \\ \frac{1}{\sigma_{X_k}^2 \sigma_{X_1}^2} \text{cov}(Y_k, X_k) \text{cov}(Y_1, X_1) & \cdots & \frac{1}{\sigma_{X_k}^2} \text{cov}^2(Y_k, X_k) \end{bmatrix} \right| \quad (41)
\end{aligned}$$

We use the notation  $\mathbf{v} = \left[ \frac{1}{\sigma_{X_1}^2} \text{cov}(Y_1, X_1) \quad \cdots \quad \frac{1}{\sigma_{X_k}^2} \text{cov}(Y_k, X_k) \right]^T$ , and  $\mathbf{V} = \text{diag}(\frac{1}{\sigma_{X_1}^2} \text{cov}^2(Y_1, X_1), \dots, \frac{1}{\sigma_{X_k}^2} \text{cov}^2(Y_k, X_k))$ . And utilize the rule of determinants of sums [35], then we have:

$$\begin{aligned}
|\Sigma_{\mathbf{Y}} - \Sigma_{\mathbf{Y}(\mathbf{X}+\epsilon)} \Sigma_{\mathbf{X}+\epsilon}^{-1} \Sigma_{(\mathbf{X}+\epsilon)\mathbf{Y}}| &= |(\Sigma_{\mathbf{Y}} - \mathbf{V}) + \lambda \mathbf{v}\mathbf{v}^T| \\
&= |\Sigma_{\mathbf{Y}} - \mathbf{V}| + \lambda \mathbf{v}^T (\Sigma_{\mathbf{Y}} - \mathbf{V})^* \mathbf{v} \quad (42)
\end{aligned}$$

where  $(\Sigma_{\mathbf{Y}} - \mathbf{V})^*$  is the adjoint of the matrix  $(\Sigma_{\mathbf{Y}} - \mathbf{V})$ . For simplicity, we can rewrite  $|\Sigma_{\mathbf{Y}} - \Sigma_{\mathbf{Y}(\mathbf{X}+\epsilon)} \Sigma_{\mathbf{X}+\epsilon}^{-1} \Sigma_{(\mathbf{X}+\epsilon)\mathbf{Y}}|$  as:

$$\begin{aligned}
& |\Sigma_{\mathbf{Y}} - \Sigma_{\mathbf{Y}(\mathbf{X}+\epsilon)} \Sigma_{\mathbf{X}+\epsilon}^{-1} \Sigma_{(\mathbf{X}+\epsilon)\mathbf{Y}}| \\
&= \prod_{i=1}^k \left( \sigma_{Y_i}^2 - \text{cov}^2(Y_i, X_i) \frac{1}{\sigma_{X_i}^2} \right) + \Omega \quad (43)
\end{aligned}$$

where  $\Omega = \lambda \mathbf{v}^T (\Sigma_{\mathbf{Y}} - \mathbf{V})^* \mathbf{v}$ . The specific value of  $\Omega$  can be obtained as:

$$\Omega = \lambda \begin{bmatrix} \frac{1}{\sigma_{X_1}^2} \text{cov}(Y_1, X_1) & \cdots & \frac{1}{\sigma_{X_k}^2} \text{cov}(Y_k, X_k) \end{bmatrix} \begin{bmatrix} V_{11} & & \\ & \ddots & \\ & & V_{kk} \end{bmatrix} \begin{bmatrix} \frac{1}{\sigma_{X_1}^2} \text{cov}(Y_1, X_1) \\ \vdots \\ \frac{1}{\sigma_{X_k}^2} \text{cov}(Y_k, X_k) \end{bmatrix} \quad (44)$$

where the elements  $V_{ii}, i \in [1, k]$  are minors of the matrix and expressed as:

$$V_{ii} = \prod_{j=1, j \neq i}^k \left[ \sigma_{Y_j}^2 - \frac{1}{\sigma_{X_j}^2} \text{cov}^2(X_j, Y_j) \right] \quad (45)$$

After some necessary steps, Equation 44 is reduced to:

$$\begin{aligned}\Omega &= \lambda \sum_{i=1}^k \frac{\frac{1}{\sigma_{X_i}^4} \text{cov}^2(Y_i, X_i) \prod_{j=1}^k (\sigma_{Y_j}^2 - \text{cov}^2(Y_j, X_j) \frac{1}{\sigma_{X_j}^2})}{(\sigma_{Y_i}^2 - \text{cov}^2(Y_i, X_i) \frac{1}{\sigma_{X_i}^2})} \\ &= \lambda \prod_{i=1}^k (\sigma_{Y_i}^2 - \text{cov}^2(Y_i, X_i) \frac{1}{\sigma_{X_i}^2}) \cdot \sum_{i=1}^k \frac{\text{cov}^2(X_i, Y_i)}{\sigma_{X_i}^2 (\sigma_{X_i}^2 \sigma_{Y_i}^2 - \text{cov}^2(X_i, Y_i))}\end{aligned}\quad (46)$$

Substitute Equation 46 into Equation 43, we can get:

$$\begin{aligned}& |\Sigma_{\mathbf{Y}} - \Sigma_{\mathbf{Y}(\mathbf{X}+\epsilon)} \Sigma_{\mathbf{X}+\epsilon}^{-1} \Sigma_{(\mathbf{X}+\epsilon)\mathbf{Y}}| \\ &= \prod_{i=1}^k (\sigma_{Y_i}^2 - \text{cov}^2(Y_i, X_i) \frac{1}{\sigma_{X_i}^2}) \cdot (1 + \lambda \sum_{i=1}^k \frac{\text{cov}^2(X_i, Y_i)}{\sigma_{X_i}^2 (\sigma_{X_i}^2 \sigma_{Y_i}^2 - \text{cov}^2(X_i, Y_i))})\end{aligned}\quad (47)$$

Accordingly,  $|\Sigma_{\mathbf{Y}} - \Sigma_{\mathbf{Y}\mathbf{X}} \Sigma_{\mathbf{X}}^{-1} \Sigma_{\mathbf{X}\mathbf{Y}}|$  is:

$$|\Sigma_{\mathbf{Y}} - \Sigma_{\mathbf{Y}\mathbf{X}} \Sigma_{\mathbf{X}}^{-1} \Sigma_{\mathbf{X}\mathbf{Y}}| = \prod_{i=1}^k (\sigma_{Y_i}^2 - \frac{1}{\sigma_{X_i}^2} \text{cov}^2(X_i, Y_i)) \quad (48)$$

As a result,  $\frac{|\Sigma_{\mathbf{Y}|\mathbf{X}+\epsilon}|}{|\Sigma_{\mathbf{Y}|\mathbf{X}}|}$  is expressed as:

$$\frac{|\Sigma_{\mathbf{Y}|\mathbf{X}}|}{|\Sigma_{\mathbf{Y}|\mathbf{X}+\epsilon}|} = \frac{\prod_{i=1}^k (\sigma_{Y_i}^2 - \frac{1}{\sigma_{X_i}^2} \text{cov}^2(X_i, Y_i))}{\prod_{i=1}^k (\sigma_{Y_i}^2 - \text{cov}^2(Y_i, X_i) \frac{1}{\sigma_{X_i}^2}) \cdot (1 + \lambda \sum_{i=1}^k \frac{\text{cov}^2(X_i, Y_i)}{\sigma_{X_i}^2 (\sigma_{X_i}^2 \sigma_{Y_i}^2 - \text{cov}^2(X_i, Y_i))}} \quad (49)$$

Combine Equations 49 and 2 together, the mutual information is expressed as:

$$\begin{aligned}MI(\mathcal{T}, \epsilon) &= \frac{1}{2} \log \frac{\prod_{i=1}^k (\sigma_{Y_i}^2 - \frac{1}{\sigma_{X_i}^2} \text{cov}^2(X_i, Y_i))}{\prod_{i=1}^k (\sigma_{Y_i}^2 - \text{cov}^2(Y_i, X_i) \frac{1}{\sigma_{X_i}^2}) \cdot (1 + \lambda \sum_{i=1}^k \frac{\text{cov}^2(X_i, Y_i)}{\sigma_{X_i}^2 (\sigma_{X_i}^2 \sigma_{Y_i}^2 - \text{cov}^2(X_i, Y_i))}} \\ &= \frac{1}{2} \log \frac{1}{1 + \lambda \sum_{i=1}^k \frac{\text{cov}^2(X_i, Y_i)}{\sigma_{X_i}^2 (\sigma_{X_i}^2 \sigma_{Y_i}^2 - \text{cov}^2(X_i, Y_i))}}\end{aligned}\quad (50)$$

It is difficult to tell that Equation 49 is greater or smaller than 1 directly. But one thing for sure is that when there is no Gaussian noise, Equation 49 equals 1. However, we can use another way to compare the numerator and denominator of Equation 49. Instead, we compare the numerator and denominator using subtraction. Let:

$$\begin{aligned}f(\sigma_\epsilon^2) &= 1 - (1 + \lambda \sum_{i=1}^k \frac{\text{cov}^2(X_i, Y_i)}{\sigma_{X_i}^2 (\sigma_{X_i}^2 \sigma_{Y_i}^2 - \text{cov}^2(X_i, Y_i))}) \\ &= -\lambda \sum_{i=1}^k \frac{\text{cov}^2(X_i, Y_i)}{\sigma_{X_i}^2 (\sigma_{X_i}^2 \sigma_{Y_i}^2 - \text{cov}^2(X_i, Y_i))} \\ &= -\frac{\sigma_\epsilon^2}{1 + \sum_{i=1}^k \frac{1}{\sigma_{X_i}^2}} \sum_{i=1}^k \frac{\text{cov}^2(X_i, Y_i)}{\sigma_{X_i}^2 (\sigma_{X_i}^2 \sigma_{Y_i}^2 - \text{cov}^2(X_i, Y_i))}\end{aligned}\quad (51)$$

Obviously, the variance  $\sigma_\epsilon^2$  of the Gaussian noise control the result of  $f(\sigma_\epsilon)$ , while the mean  $\mu_\epsilon$  has no influence. When  $\sigma_\epsilon$  approaching 0, we have:

$$\lim_{\sigma_\epsilon^2 \rightarrow 0} f(\sigma_\epsilon^2) = 0 \quad (52)$$

To determine if Gaussian noise can be positive noise, we need to determine whether the mutual information is large or smaller than 0:

$$\begin{cases} \frac{|\Sigma_{\mathbf{Y}|\mathbf{X}}|}{|\Sigma_{\mathbf{Y}|\mathbf{X}+\epsilon}|} > 1 & \text{if } f(\sigma_\epsilon^2) > 0 \\ \frac{|\Sigma_{\mathbf{Y}|\mathbf{X}}|}{|\Sigma_{\mathbf{Y}|\mathbf{X}+\epsilon}|} \leq 1 & \text{if } f(\sigma_\epsilon^2) \leq 0 \end{cases} \quad (53)$$

Combine the Equations 36 and 53, we can get the conclusion:

$$\begin{cases} MI(\mathcal{T}, \epsilon) > 0 & \text{if } f(\sigma_\epsilon^2) > 0 \\ MI(\mathcal{T}, \epsilon) \leq 0 & \text{if } f(\sigma_\epsilon^2) \leq 0 \end{cases} \quad (54)$$

From the above equations, the sign of the mutual information is determined by the statistical properties of the data samples and labels. Since  $\epsilon^2 \geq 0$  and  $\sum_{i=1}^k \frac{1}{\sigma_{X_i}^2} \geq 0$ , we have a deep dive into the residual part, i.e.,

$$\sum_{i=1}^k \frac{\text{cov}^2(X_i, Y_i)}{\sigma_{X_i}^2 (\sigma_{X_i}^2 \sigma_{Y_i}^2 - \text{cov}^2(X_i, Y_i))} = \sum_{i=1}^k \frac{\text{cov}^2(X_i, Y_i)}{\sigma_{X_i}^4 \sigma_{Y_i}^2 (1 - \rho_{X_i Y_i}^2)} \quad (55)$$

where  $\rho_{X_i Y_i}$  is the correlation coefficient, and  $\rho_{X_i Y_i}^2 \in [0, 1]$ . As a result, the sign of the mutual information in the Gaussian noise case is negative. We can conclude that Gaussian noise added to the images is harmful to the task.

### A.1.2 Inject Gaussian Noise in Latent Space

In this case, the task entropy is formulated as:

$$H(\mathcal{T}; \mathbf{X} + \epsilon) = H(\mathbf{Y}; \mathbf{X} + \epsilon) - H(\mathbf{X}). \quad (56)$$

Thus, the mutual information of injecting Gaussian noise can be formulated as:

$$\begin{aligned} MI(\mathcal{T}, \epsilon) &= H(\mathbf{Y}; \mathbf{X}) - H(\mathbf{X}) - (H(\mathbf{Y}; \mathbf{X} + \epsilon) - H(\mathbf{X})) \\ &= H(\mathbf{Y}; \mathbf{X}) - H(\mathbf{Y}; \mathbf{X} + \epsilon) \end{aligned} \quad (57)$$

Borrow the equations from the case of Gaussian noise added the original image, we have:

$$\begin{aligned} MI(\mathcal{T}, \epsilon) &= H(\mathbf{Y}; \mathbf{X}) - H(\mathbf{Y}; \mathbf{X} + \epsilon) \\ &= \frac{1}{2} \log \frac{|\Sigma_{\mathbf{X}}| |\Sigma_{\mathbf{Y}} - \Sigma_{\mathbf{Y}\mathbf{X}} \Sigma_{\mathbf{X}}^{-1} \Sigma_{\mathbf{X}\mathbf{Y}}|}{|\Sigma_{\mathbf{X}+\epsilon}| |\Sigma_{\mathbf{Y}} - \Sigma_{\mathbf{Y}\mathbf{X}} \Sigma_{\mathbf{X}+\epsilon}^{-1} \Sigma_{\mathbf{X}\mathbf{Y}}|} \\ &= \frac{1}{2} \log \frac{1}{(1 + \sigma_\epsilon^2 \sum_{i=1}^k \frac{1}{\sigma_{X_i}^2}) (1 + \lambda \sum_{i=1}^k \frac{\text{cov}^2(X_i, Y_i)}{\sigma_{X_i}^2 (\sigma_{X_i}^2 \sigma_{Y_i}^2 - \text{cov}^2(X_i, Y_i))}} \end{aligned} \quad (58)$$

Obviously, injecting Gaussian noise into the latent space is harmful to the task.

## A.2 Influence of Linear Transform Noise on Task Entropy

In our work, the linear transform noise refers to an image or the latent representation of an image that is perturbed by the combination of other images or latent representations of other images.

### A.2.1 Add Linear Transform Noise to Original Images

The task entropy with linear transform noise can be formulated as:

$$\begin{aligned} H(\mathcal{T}; \mathbf{X} + Q\mathbf{X}) &= - \sum_{\mathbf{Y} \in \mathcal{Y}} p(\mathbf{Y} | \mathbf{X} + Q\mathbf{X}) \log p(\mathbf{Y} | \mathbf{X} + Q\mathbf{X}) \\ &= - \sum_{\mathbf{Y} \in \mathcal{Y}} p(\mathbf{Y} | (I + Q)\mathbf{X}) \log p(\mathbf{Y} | (I + Q)\mathbf{X}) \end{aligned} \quad (59)$$

where  $I$  is an identity matrix, and  $Q$  is derived from  $I$  using elementary row operations. The conditional distribution of  $\mathbf{Y}$  given  $\mathbf{X} + Q\mathbf{X}$  is also multivariate subjected to the normal distribution, which can be formulated as:

$$\mathbf{Y} | (I + Q)\mathbf{X} \sim \mathcal{N}(\mathbb{E}(\mathbf{Y} | (I + Q)\mathbf{X}), \text{var}(\mathbf{Y} | (I + Q)\mathbf{X})) \quad (60)$$

The linear transform on  $\mathbf{X}$  does not change the distribution of the  $\mathbf{X}$ . It is not difficult to obtain:

$$\mu_{\mathbf{Y} | (I+Q)\mathbf{X}} = \mu_{\mathbf{Y}} + \Sigma_{\mathbf{Y}\mathbf{X}} \Sigma_{\mathbf{X}}^{-1} (I + Q)^{-1} ((I + Q)\mathbf{X} - (I + Q)\mu_{\mathbf{X}}) \quad (61)$$

$$\Sigma_{(\mathbf{Y}|(I+Q)\mathbf{X})} = \Sigma_{\mathbf{Y}} - \Sigma_{\mathbf{Y}\mathbf{X}}\Sigma_{\mathbf{X}}^{-1}\Sigma_{\mathbf{X}\mathbf{Y}} \quad (62)$$

Thus, the variation of task entropy adding linear transform noise can be formulated as:

$$\begin{aligned} MI(\mathcal{T}, Q\mathbf{X}) &= H(\mathcal{T}; \mathbf{X}) - H(\mathcal{T}; \mathbf{X} + Q\mathbf{X}) \\ &= \frac{1}{2} \log |\Sigma_{\mathbf{Y}|\mathbf{X}}| - \frac{1}{2} \log |\Sigma_{\mathbf{Y}|\mathbf{X}+Q\mathbf{X}}| \\ &= \frac{1}{2} \log \frac{|\Sigma_{\mathbf{Y}|\mathbf{X}}|}{|\Sigma_{\mathbf{Y}|\mathbf{X}+Q\mathbf{X}}|} \\ &= \frac{1}{2} \log \frac{|\Sigma_{\mathbf{Y}} - \Sigma_{\mathbf{Y}\mathbf{X}}\Sigma_{\mathbf{X}}^{-1}\Sigma_{\mathbf{X}\mathbf{Y}}|}{|\Sigma_{\mathbf{Y}} - \Sigma_{\mathbf{Y}\mathbf{X}}\Sigma_{\mathbf{X}}^{-1}\Sigma_{\mathbf{X}\mathbf{Y}}|} \\ &= 0 \end{aligned} \quad (63)$$

The mutual information of 0 indicates that the implementation of linear transformation to the original images could not reduce the complexity of the task.

### A.2.2 Inject Linear Transform Noise in Latent Space

The mutual information of injecting linear transform noise can be formulated as:

$$\begin{aligned} MI(\mathcal{T}, Q\mathbf{X}) &= H(\mathbf{Y}; \mathbf{X}) - H(\mathbf{X}) - (H(\mathbf{Y}; \mathbf{X} + Q\mathbf{X}) - H(\mathbf{X})) \\ &= H(\mathbf{Y}; \mathbf{X}) - H(\mathbf{Y}; \mathbf{X} + Q\mathbf{X}) \\ &= \frac{1}{2} \log \frac{|\Sigma_{\mathbf{X}}||\Sigma_{\mathbf{Y}} - \Sigma_{\mathbf{Y}\mathbf{X}}\Sigma_{\mathbf{X}}^{-1}\Sigma_{\mathbf{X}\mathbf{Y}}|}{|\Sigma_{(I+Q)\mathbf{X}}||\Sigma_{\mathbf{Y}} - \Sigma_{\mathbf{Y}\mathbf{X}}\Sigma_{\mathbf{X}}^{-1}\Sigma_{\mathbf{X}\mathbf{Y}}|} \\ &= \frac{1}{2} \log \frac{1}{|I + Q|^2} \\ &= -\log |I + Q| \end{aligned} \quad (64)$$

Since we want the mutual information to be greater than 0, we can formulate Equation 64 as an optimization problem:

$$\begin{aligned} &\max_Q MI(\mathcal{T}, Q\mathbf{X}) \\ &s.t. \text{rank}(I + Q) = k \\ &\quad Q \sim I \\ &\quad [I + Q]_{ii} \geq [I + Q]_{ij}, i \neq j \\ &\quad \|[I + Q]_i\|_1 = 1 \end{aligned} \quad (65)$$

where  $\sim$  means the row equivalence. The key to determining whether the linear transform is positive noise or not lies in the matrix of  $Q$ . The most important step is to ensure that  $I + Q$  is reversible, which is  $|(I + Q)| \neq 0$ . For this, we need to investigate what leads  $I + Q$  to be rank-deficient. The third constraint is to make the trained classifier get enough information about a specific image and correctly predict the corresponding label. For example, for an image  $X_1$  perturbed by another image  $X_2$ , the classifier obtained dominant information from  $X_1$  so that it can predict the label  $Y_1$ . However, if the perturbed image  $X_2$  is dominant, the classifier can hardly predict the correct label  $Y_1$ . The fourth constraint is the normalization of latent representations.

**Rank Deficiency Cases** To avoid causing a rank deficiency of  $I + Q$ , we need to figure out the conditions that lead to rank deficiency. Here we show a simple case causing the rank deficiency. When the matrix  $Q$  is a backward identity matrix [22],

$$Q_{i,j} = \begin{cases} 1, & i + j = k + 1 \\ 0, & i + j \neq k + 1 \end{cases} \quad (66)$$

i.e.,

$$Q = \begin{bmatrix} 0 & 0 & \dots & 0 & 0 & 1 \\ 0 & 0 & \dots & 0 & 1 & 0 \\ \vdots & \vdots & & \vdots & \vdots & \vdots \\ 0 & 1 & \dots & 0 & 0 & 0 \\ 1 & 0 & \dots & 0 & 0 & 0 \end{bmatrix} \quad (67)$$

then  $(I + Q)$  will be:

$$I + Q = \begin{bmatrix} 1 & 0 & \dots & 0 & 0 & 1 \\ 0 & 1 & \dots & 0 & 1 & 0 \\ \vdots & \vdots & & \vdots & \vdots & \vdots \\ 0 & 1 & \dots & 0 & 1 & 0 \\ 1 & 0 & \dots & 0 & 0 & 1 \end{bmatrix} \quad (68)$$

Thus,  $I + Q$  will be rank-deficient when  $Q$  is a backward identity. In fact, when the following constraints are satisfied, the  $I + Q$  will be rank-deficient:

$$\text{HermiteForm}(I + Q)_i = \mathbf{0}, \quad \exists i \in [1, k] \quad (69)$$

where index  $i$  is the row index, in this paper, the row index starts from 1, and HermiteForm is the Hermite normal form [24].

**Full Rank Cases** Except for the rank deficiency cases,  $I + Q$  has full rank and is reversible. Since  $Q$  is a row equivalent to the identity matrix, we need to introduce the three types of elementary row operations as follows [51].

- ▷ 1 **Row Swap** Exchange rows.  
Row swap here allows exchanging any number of rows. This is slightly different from the original one that only allows any two rows exchange since following the original row swap will lead to a rank deficiency. When the  $Q$  is derived from  $I$  with **Row Swap**, it will break the third constraint. Therefore, **Row Swap** merely is considered harmful and would degrade the deep model.
- ▷ 2 **Scalar Multiplication** Multiply any row by a constant  $\beta$ . This breaks the fourth constraint, thus degrading the deep models.
- ▷ 3 **Row Sum** Add a multiple of one row to another row. Then the matrix  $I + Q$  would be like:

$$\begin{aligned} I + Q &= \begin{bmatrix} 1 & & & & & \\ & \cdot & & & & \\ & & \cdot & & & \\ & & & \cdot & & \\ & & & & 1 & \\ & & & & & 1 \end{bmatrix} + \begin{bmatrix} 1 & & & & & \\ & \cdot & & & & \\ & & \cdot & & & \\ & & & \cdot & & \\ & & & & \beta & \\ & & & & & \cdot \\ & & & & & & 1 \end{bmatrix} \\ &= \begin{bmatrix} 2 & & & & & \\ & \cdot & \beta & & & \\ & & \cdot & & & \\ & & & \cdot & & \\ & & & & \cdot & \\ & & & & & 2 \end{bmatrix} \end{aligned} \quad (70)$$

where  $\beta$  can be at a random position beside the diagonal. As we can see from the simple example, **Row Sum** breaks the fourth constraint and make mutual information smaller than 0.

From the above discussion, none of the single elementary row operations can guarantee positive effects on deep models.

However, if we combine the elementary row operations, it is possible to make the mutual information greater than 0 as well as satisfy the constraints. For example, we combine the **Row Swap** and **Scalar Multiplication** to generate the  $Q$ :

$$\begin{aligned} I + Q &= \begin{bmatrix} 1 & & & & & \\ & \cdot & & & & \\ & & \cdot & & & \\ & & & \cdot & & \\ & & & & 1 & \\ & & & & & 1 \end{bmatrix} + \begin{bmatrix} -0.5 & 0.5 & & & & \\ & \cdot & & & & \\ & & \cdot & & & \\ & & & \cdot & & \\ & & & & \cdot & \\ & & & & & \cdot & 0.5 \\ 0.5 & & & & & & -0.5 \end{bmatrix} \\ &= \begin{bmatrix} 0.5 & 0.5 & & & & \\ & \cdot & & & & \\ & & \cdot & & & \\ & & & \cdot & & \\ & & & & \cdot & \\ & & & & & \cdot & 0.5 \\ 0.5 & & & & & & 0.5 \end{bmatrix} \end{aligned} \quad (71)$$

In this case,  $MI(\mathcal{T}, Q\mathbf{X}) > 0$  when  $Q = -0.5I$ . The constraints are satisfied. This is just a simple case that adding linear transform noise that benefits deep models. Actually, there exists a design space of  $Q$  that within the design space, deep models can reduce task entropy by injecting linear transform noise. To this end, we demonstrate that linear transform can be positive noise.

### A.3 Influence of Salt-and-pepper Noise on Task Entropy

Salt-and-pepper noise is a common type of noise that can occur in images due to various factors, such as signal transmission errors, faulty sensors, or other environmental factors [8]. Salt-and-pepper noise is often considered to be an independent process because it is a type of random noise that affects individual pixels in an image independently of each other [19].

#### A.3.1 Add Salt-and-pepper Noise to Original Images

The task entropy with salt-and-pepper noise is rewritten as:

$$H(\mathcal{T}; \mathbf{X}\epsilon) = - \sum_{\mathbf{Y} \in \mathcal{Y}} p(\mathbf{Y}|\mathbf{X}\epsilon) \log p(\mathbf{Y}|\mathbf{X}\epsilon) \quad (72)$$

Since  $\epsilon$  is independent of  $\mathbf{X}$  and  $\mathbf{Y}$ , the above equation can be expanded as:

$$\begin{aligned} H(\mathcal{T}; \mathbf{X}\epsilon) &= - \sum_{\mathbf{Y} \in \mathcal{Y}} \frac{p(\mathbf{Y}, \mathbf{X}\epsilon)}{p(\mathbf{X})p(\epsilon)} \log \frac{p(\mathbf{Y}, \mathbf{X}\epsilon)}{p(\mathbf{X})p(\epsilon)} \\ &= - \sum_{\mathbf{Y} \in \mathcal{Y}} \frac{p(\mathbf{Y}, \mathbf{X})p(\epsilon)}{p(\mathbf{X})p(\epsilon)} \log \frac{p(\mathbf{Y}, \mathbf{X})p(\epsilon)}{p(\mathbf{X})p(\epsilon)} \\ &= - \sum_{\mathbf{Y} \in \mathcal{Y}} p(\mathbf{Y}|\mathbf{X}) \log p(\mathbf{Y}|\mathbf{X}) \end{aligned} \quad (73)$$

where

$$\begin{aligned} p(\mathbf{X}\epsilon, \mathbf{Y}) &= p(\mathbf{X}\epsilon|\mathbf{Y})p(\mathbf{Y}) \\ &= p(\mathbf{X}|\mathbf{Y})p(\epsilon|\mathbf{Y})p(\mathbf{Y}) \\ &= p(\mathbf{X}|\mathbf{Y})p(\epsilon)p(\mathbf{Y}) \\ &= p(\mathbf{X}, \mathbf{Y})p(\epsilon) \end{aligned} \quad (74)$$

Therefore, the mutual information with salt-and-pepper noise is:

$$MI(\mathcal{T}, \epsilon) = H(\mathcal{T}; \mathbf{X}) - H(\mathcal{T}; \mathbf{X}\epsilon) = 0 \quad (75)$$

Salt-and-pepper noise can not help reduce the complexity of the task, and therefore, it is considered a type of pure detrimental noise.

#### A.3.2 Add Salt-and-pepper Noise in Latent Space

The mutual information of injecting salt-and-pepper noise can be formulated as:

$$\begin{aligned} MI(\mathcal{T}, \epsilon) &= H(\mathbf{Y}; \mathbf{X}) - H(\mathbf{X}) - (H(\mathbf{Y}; \mathbf{X}\epsilon) - H(\mathbf{X})) \\ &= H(\mathbf{Y}; \mathbf{X}) - H(\mathbf{Y}; \mathbf{X}\epsilon) \\ &= - \sum_{\mathbf{X} \in \mathcal{X}} \sum_{\mathbf{Y} \in \mathcal{Y}} p(\mathbf{X}, \mathbf{Y}) \log p(\mathbf{X}, \mathbf{Y}) - \sum_{\mathbf{X} \in \mathcal{X}} \sum_{\mathbf{Y} \in \mathcal{Y}} \sum_{\epsilon \in \mathcal{E}} p(\mathbf{X}\epsilon, \mathbf{Y}) \log p(\mathbf{X}\epsilon, \mathbf{Y}) \\ &= \mathbb{E} \left[ \log \frac{1}{p(\mathbf{X}, \mathbf{Y})} \right] - \mathbb{E} \left[ \log \frac{1}{p(\mathbf{X}\epsilon, \mathbf{Y})} \right] \\ &= \mathbb{E} \left[ \log \frac{1}{p(\mathbf{X}, \mathbf{Y})} \right] - \mathbb{E} \left[ \log \frac{1}{p(\mathbf{X}, \mathbf{Y})} \right] - \mathbb{E} \left[ \log \frac{1}{p(\epsilon)} \right] \\ &= - \mathbb{E} \left[ \log \frac{1}{p(\epsilon)} \right] \\ &= - H(\epsilon) \end{aligned} \quad (76)$$

The mutual information is smaller than 0, therefore, the salt-and-pepper is a pure detrimental noise to the latent representations.

From the discussion in this section, we can draw conclusions that **Linear Transform Noise** can be positive under certain conditions, while **Gaussian Noise** and **Salt-and-pepper Noise** are harmful noise. From the above analysis, the conditions that satisfy positive noise are forming a design space. Exploring the positive noise space is an important topic for future work.

## B Optimal Quality Matrix of Linear Transform Noise

The optimal quality matrix should maximize the mutual information, therefore theoretically define the minimized task complexity. The optimization problem as formulated in Equation 15 is:

$$\begin{aligned}
& \max_Q -\log |I + Q| \\
& s.t. \text{rank}(I + Q) = k \\
& \quad Q \sim I \\
& \quad [I + Q]_{ii} \geq [I + Q]_{ij}, i \neq j \\
& \quad \|[I + Q]_i\|_1 = 1
\end{aligned} \tag{77}$$

Maximizing the mutual information is to minimize the determinant of the matrix sum of  $I$  and  $Q$ . A simple but straight way is to design the matrix  $Q$  that makes the elements in  $I + Q$  equal, i.e.,

$$I + Q = \begin{bmatrix} 1/k & \cdots & 1/k \\ \vdots & \cdots & \vdots \\ 1/k & \cdots & 1/k \end{bmatrix} \tag{78}$$

The determinant of the above equation is 0, but it breaks the first constraint of  $\text{rank}(I + Q) = k$ . However, by adding a small constant into the diagonal, and minus another constant by other elements, we can get:

$$I + Q = \begin{bmatrix} 1/k + c_1 & \cdots & & 1/k - c_2 \\ 1/k - c_2 & \ddots & & \vdots \\ \vdots & & \ddots & 1/k - c_2 \\ 1/k - c_2 & \cdots & 1/k - c_2 & 1/k + c_1 \end{bmatrix} \tag{79}$$

Under the constraints, we can obtain the two constants that fulfill the requirements:

$$c_1 = \frac{k-1}{k(k+1)}, \quad c_2 = \frac{1}{k(k+1)} \tag{80}$$

Therefore, the corresponding  $Q$  is:

$$Q_{optimal} = \text{diag} \left( \frac{1}{k+1} - 1, \dots, \frac{1}{k+1} - 1 \right) + \frac{1}{k+1} \mathbf{1}_{k \times k} \tag{81}$$

and the corresponding  $I + Q$  is:

$$I + Q = \begin{bmatrix} 2/(k+1) & \cdots & & 1/(k+1) \\ 1/(k+1) & \ddots & & \vdots \\ \vdots & & \ddots & 1/(k+1) \\ 1/(k+1) & \cdots & 1/(k+1) & 2/(k+1) \end{bmatrix} \tag{82}$$

As a result, the determinant of optimal  $I + Q$  can be obtained by following the identical procedure as Equation 42:

$$|I + Q| = \frac{1}{(k+1)^{k-1}} \tag{83}$$

The upper boundary of mutual information of linear transform noise is determined:

$$MI(\mathcal{T}, Q\mathbf{X})_{upper} = (k-1) \log(k+1) \tag{84}$$

Table 8: Details of ResNet Models. The columns "18-layer", "34-layer", "50-layer", and "101-layer" show the specifications of ResNet-18, ResNet-34, ResNet-50, and ResNet-101, separately.

Layer name	Output size	18-layer	34-layer	50-layer	101-layer
conv1	$112 \times 112$	$7 \times 7, 64, \text{stride } 2$			
		$3 \times 3, \text{max pool, stride } 2$			
conv2_x	$56 \times 56$	$\begin{bmatrix} 3 \times 3 & 64 \\ 3 \times 3 & 64 \end{bmatrix} \times 2$	$\begin{bmatrix} 3 \times 3 & 64 \\ 3 \times 3 & 64 \end{bmatrix} \times 3$	$\begin{bmatrix} 1 \times 1 & 64 \\ 3 \times 3 & 64 \\ 1 \times 1 & 256 \end{bmatrix} \times 3$	$\begin{bmatrix} 1 \times 1 & 64 \\ 3 \times 3 & 64 \\ 1 \times 1 & 256 \end{bmatrix} \times 3$
conv3_x	$28 \times 28$	$\begin{bmatrix} 3 \times 3 & 128 \\ 3 \times 3 & 128 \end{bmatrix} \times 2$	$\begin{bmatrix} 3 \times 3 & 128 \\ 3 \times 3 & 128 \end{bmatrix} \times 4$	$\begin{bmatrix} 1 \times 1 & 128 \\ 3 \times 3 & 128 \\ 1 \times 1 & 512 \end{bmatrix} \times 4$	$\begin{bmatrix} 1 \times 1 & 128 \\ 3 \times 3 & 128 \\ 1 \times 1 & 512 \end{bmatrix} \times 4$
conv4_x	$14 \times 14$	$\begin{bmatrix} 3 \times 3 & 256 \\ 3 \times 3 & 256 \end{bmatrix} \times 2$	$\begin{bmatrix} 3 \times 3 & 256 \\ 3 \times 3 & 256 \end{bmatrix} \times 6$	$\begin{bmatrix} 1 \times 1 & 256 \\ 3 \times 3 & 256 \\ 1 \times 1 & 1024 \end{bmatrix} \times 6$	$\begin{bmatrix} 1 \times 1 & 256 \\ 3 \times 3 & 256 \\ 1 \times 1 & 1024 \end{bmatrix} \times 23$
conv5_x	$7 \times 7$	$\begin{bmatrix} 3 \times 3 & 512 \\ 3 \times 3 & 512 \end{bmatrix} \times 2$	$\begin{bmatrix} 3 \times 3 & 512 \\ 3 \times 3 & 512 \end{bmatrix} \times 3$	$\begin{bmatrix} 1 \times 1 & 512 \\ 3 \times 3 & 512 \\ 1 \times 1 & 2048 \end{bmatrix} \times 3$	$\begin{bmatrix} 1 \times 1 & 512 \\ 3 \times 3 & 512 \\ 1 \times 1 & 2048 \end{bmatrix} \times 3$
	$1 \times 1$	average pool, 1000-d fc, softmax			
Params		11M	22M	26M	45M

Table 9: Details of ViT Models. Each row shows the specifications of a kind of ViT model. ViT-T, ViT-S, ViT-B, and ViT-L represent ViT Tiny, ViT Small, ViT Base, and ViT Large, separately.

ViT Model	Layers	Hidden size	MLP size	Heads	Params
ViT-T	12	192	768	3	5.7M
ViT-S	12	384	1536	6	22M
ViT-B	12	768	3072	12	86M
ViT-L	12	1024	4096	16	307M

Table 10: Variants of ViT with different kinds of noise on TinyImageNet. Vanilla means the vanilla model without noise. Accuracy is shown in percentage. Gaussian noise used here is subjected to standard normal distribution. Linear transform noise used in this table is designed to be positive noise. The difference is shown in the bracket.

Model	DeiT	SwinTransformer	BeiT	ConViT
Vanilla	85.02 (+0.00)	90.84 (+0.00)	88.64 (+0.00)	90.69 (+0.00)
+ Gaussian Noise	84.70 (-0.32)	90.34 (-0.50)	88.40 (-0.24)	90.40 (-0.29)
+ Linear Transform Noise	<b>86.50 (+1.48)</b>	<b>95.68 (+4.84)</b>	<b>91.78 (+3.14)</b>	<b>93.07 (+2.38)</b>
+ Salt-and-pepper Noise	84.03 (-1.01)	87.12 (-3.72)	42.18 (-46.46)	89.93 (-0.76)
Params.	86M	87M	86M	86M

Table 11: ResNet with different kinds of noise on TinyImageNet. Vanilla means the vanilla model without noise. Accuracy is shown in percentage. Gaussian noise used here is subjected to standard normal distribution. Linear transform noise used in this table is designed to be positive noise. The difference is shown in the bracket.

Model	ResNet-18	ResNet-34	ResNet-50	ResNet-101
Vanilla	64.01 (+0.00)	67.04 (+0.00)	69.47 (+0.00)	70.66 (+0.00)
+ Gaussian Noise	63.23 (-0.78)	65.71 (-1.33)	68.17 (-1.30)	69.13 (-1.53)
+ Linear Transform Noise	<b>73.32 (+9.31)</b>	<b>76.70 (+9.66)</b>	<b>76.88 (+7.41)</b>	<b>77.30 (+6.64)</b>
+ Salt-and-pepper Noise	55.97 (-8.04)	63.52 (-3.52)	49.42 (-20.25)	53.88 (-16.78)

Table 12: ViT with different kinds of noise on TinyImageNet. Vanilla means the vanilla model without injecting noise. Accuracy is shown in percentage. Gaussian noise used here is subjected to standard normal distribution. Linear transform noise used in this table is designed to be positive noise. The difference is shown in the bracket. Note **ViT-L is overfitting on TinyImageNet** [15] [53].

Model	ViT-T	ViT-S	ViT-B	ViT-L
Vanilla	81.75 (+0.00)	86.78 (+0.00)	90.48 (+0.00)	93.32 (+0.00)
+ Gaussian Noise	80.95 (-0.80)	85.66 (-1.12)	89.61 (-0.87)	92.31 (-1.01)
+ Linear Transform Noise	<b>82.50 (+0.75)</b>	<b>91.62 (+4.84)</b>	<b>94.92 (+4.44)</b>	<b>93.63 (+0.31)</b>
+ Salt-and-pepper Noise	79.34 (-2.41)	84.66 (-2.12)	87.45 (-3.03)	83.48 (-9.84)

## C Experimental Setting

We introduce the implementation details in this part. Model details are shown in Table 8 and 9. The image resolution is  $224 \times 224$  for all the experiments. Pre-trained models on ImageNet are used as the backbone. We train all ResNet and ViT-based models using AdamW optimizer [34]. We set the learning rate of each parameter group using a cosine annealing schedule with a minimum of  $1e - 7$ . The data augmentation for training only includes the random resized crop and normalization.

**CNN(ResNet) Setting** The training epoch is set to 100. We initialized the learning rate as 0 and linearly increase it to 0.001 after 10 warmup steps. All the experiments of CNNs are trained on a single Tesla V100 GPU with 32 GB. The batch size for ResNet18, ResNet34, ResNet50, and ResNet101 are 1024, 512, 256, and 128, respectively.

**ViT and Variants Setting** All the experiments of ViT and its variants are trained on a single machine with 8 Tesla V100 GPUs. For vanilla ViTs, including ViT-T, ViT-S, ViT-B, and ViT-L, the training epoch is set to 50 and the input patch size is  $16 \times 16$ . We initialized the learning rate as 0 and linearly increase it to 0.0001 after 10 warmup steps. We then decrease it by the cosine decay strategy. For experiments on the variants of ViT, the training epoch is set to 100 and the learning rate is set to 0.0005 with 10 warmup steps.

## D More Experiment Results

We show more experiment results of injecting positive noise to other variants of the ViT family, such as SwinTransformer, DeiT, ConViT, and BeiT, and implement them on the smaller dataset, i.e., TinyImageNet. Note, considering limited computational resources, all the experiments in the supplementary are on the TinyImageNet. The strength of positive noise is set to 0.3. The noise is injected into the last layer.

### D.1 Inject Positive Noise to Variants of ViT

As demonstrated in the paper, the positive noise can be injected into the ViT family. Therefore, in this section, we explore the influence of positive noise on the variants of the ViT. The positive noise used here is identical to that in the paper. For this, we comprehensively compare noise injection to ConViT [11], BeiT [3], DeiT [58], and Swin Transformer [32], and comparisons results are reported in Tabel 10. As expected, these variants of ViTs get benefit from the positive noise. The additional four ViT variants are at the base scale, whose parameters are listed in the table’s last row. For a fair comparison, we use identical experimental settings for each kind of experiment. For example, we use the identical setting for vanilla ConViT, ConViT with different kinds of noise. From the experimental results, we can observe that the different variants of ViT benefit from positive noise and significantly improve prediction accuracy. The results on different scale datasets and variants of the ViT family demonstrate that positive noise can universally improve the model performance by a wide margin.

### D.2 Positive Noise on TinyImageNet

We also implement experiments of ResNet and ViT on the smaller dataset TinyImageNet, and the results are shown in Table 11 and 12. As shown in the tables, positive noise also benefits the deep models on the small dataset. From the experiment results of CNN and ViT family on ImageNet and

Table 13: Comparison with SOTA methods on **Office-Home**. The best performance is marked in red.

Method	Ar2C	Ar2Pr	Ar2Re	Cl2Ar	Cl2Pr	Cl2Re	Pr2Ar	Pr2Cl	Pr2Re	Re2Ar	Re2Cl	Re2Pr	Avg.
ResNet-50 [21]	44.9	66.3	74.3	51.8	61.9	63.6	52.4	39.1	71.2	63.8	45.9	77.2	59.4
MinEnt [20]	51.0	71.9	77.1	61.2	69.1	70.1	59.3	48.7	77.0	70.4	53.0	81.0	65.8
SAFN [64]	52.0	71.7	76.3	64.2	69.9	71.9	63.7	51.4	77.1	70.9	57.1	81.5	67.3
CDAN+E [33]	54.6	74.1	78.1	63.0	72.2	74.1	61.6	52.3	79.1	72.3	57.3	82.8	68.5
DCAN [28]	54.5	75.7	81.2	67.4	74.0	76.3	67.4	52.7	80.6	74.1	59.1	83.5	70.5
BNM [10]	56.7	77.5	81.0	67.3	76.3	77.1	65.3	55.1	82.0	73.6	57.0	84.3	71.1
SHOT [30]	57.1	78.1	81.5	68.0	78.2	78.1	67.4	54.9	82.2	73.3	58.8	84.3	71.8
ATDOC-NA [31]	58.3	78.8	82.3	69.4	78.2	78.2	67.1	56.0	82.7	72.0	58.2	85.5	72.2
ViT-B [15]	54.7	83.0	87.2	77.3	83.4	85.6	74.4	50.9	87.2	79.6	54.8	88.8	75.5
TVT-B [66]	74.9	86.8	89.5	82.8	88.0	88.3	79.8	71.9	90.1	85.5	74.6	90.6	83.6
CDTrans-B [65]	68.8	85.0	86.9	81.5	87.1	87.3	79.6	63.3	88.2	82.0	66.0	90.6	80.5
SSRT-B [56]	75.2	89.0	91.1	85.1	88.3	90.0	85.0	74.2	91.3	85.7	78.6	91.8	85.4
TVT-B+PN (ours)	<b>78.3</b>	<b>90.6</b>	<b>91.9</b>	<b>87.8</b>	<b>92.1</b>	<b>91.9</b>	<b>85.8</b>	<b>78.7</b>	<b>93.0</b>	<b>88.6</b>	<b>80.6</b>	<b>93.5</b>	<b>87.7</b>

Table 14: Comparison with SOTA methods on **Visda2017**. The best performance is marked in red.

Method	plane	bycycl	bus	car	horse	knife	mcycl	person	plant	sktbrd	train	truck	Avg.
ResNet-50 [21]	55.1	53.3	61.9	59.1	80.6	17.9	79.7	31.2	81.0	26.5	73.5	8.5	52.4
DANN [18]	81.9	77.7	82.8	44.3	81.2	29.5	65.1	28.6	51.9	54.6	82.8	7.8	57.4
MinEnt [20]	80.3	75.5	75.8	48.3	77.9	27.3	69.7	40.2	46.5	46.6	79.3	16.0	57.0
SAFN [64]	93.6	61.3	84.1	70.6	94.1	79.0	91.8	79.6	89.9	55.6	89.0	24.4	76.1
CDAN+E [33]	85.2	66.9	83.0	50.8	84.2	74.9	88.1	74.5	83.4	76.0	81.9	38.0	73.9
BNM [10]	89.6	61.5	76.9	55.0	89.3	69.1	81.3	65.5	90.0	47.3	89.1	30.1	70.4
CGDM [16]	93.7	82.7	73.2	68.4	92.9	94.5	88.7	82.1	93.4	82.5	86.8	49.2	82.3
SHOT [30]	94.3	88.5	80.1	57.3	93.1	93.1	80.7	80.3	91.5	89.1	86.3	58.2	82.9
ViT-B [15]	97.7	48.1	86.6	61.6	78.1	63.4	94.7	10.3	87.7	47.7	94.4	35.5	67.1
TVT-B [66]	92.9	85.6	77.5	60.5	93.6	98.2	89.4	76.4	93.6	92.0	91.7	55.7	83.9
CDTrans-B [65]	97.1	90.5	82.4	77.5	96.6	96.1	93.6	<b>88.6</b>	<b>97.9</b>	86.9	90.3	62.8	88.4
SSRT-B [56]	<b>98.9</b>	87.6	<b>89.1</b>	<b>84.8</b>	98.3	<b>98.7</b>	<b>96.3</b>	81.1	94.9	97.9	94.5	43.1	88.8
TVT-B+PN (ours)	98.8	<b>95.5</b>	84.8	73.7	<b>98.5</b>	97.2	95.1	76.5	95.9	<b>98.4</b>	<b>98.3</b>	<b>67.2</b>	<b>90.0</b>

TinyImageNet, we can find that the positive noise has better effects on larger datasets than smaller ones. This makes sense because as shown in the section on optimal quality matrix, the upper boundary of the mutual information is determined by the size, i.e., the number of data samples, of the dataset, smaller datasets have less number of data samples, which means the upper boundary of the small datasets is lower than the large datasets. Therefore, the positive noise of linear transform noise has better influences on large than small datasets.

### D.3 Positive Noise for Domain Adaptation

Unsupervised domain adaptation (UDA) aims to learn transferable knowledge across the source and target domains with different distributions [41] [62]. There are mainly two kinds of deep neural networks for UDA, which are CNN-based and Transformer-based methods [56] [66]. Various techniques for UDA are adopted on these backbone architectures. For example, the discrepancy techniques measure the distribution divergence between source and target domains [33] [54]. Adversarial adaptation discriminates domain-invariant and domain-specific representations by playing an adversarial game between the feature extractor and a domain discriminator [18].

Recently, transformer-based methods achieved SOTA results on UDA, therefore, we evaluate the ViT-B with the positive noise on widely used UDA benchmarks. Here the positive noise is the linear transform noise identical to that used in the classification task. The positive noise is injected into the last layer of the model, the same as the classification task. The datasets include **Office Home** [61] and **VisDA2017** [42]. **Office-Home** [61] has 15,500 images of 65 classes from four domains: Artistic (Ar), Clip Art (Cl), Product (Pr), and Real-world (Rw) images. **VisDA2017** is a Synthetic-to-Real object recognition dataset, with more than 0.2 million images in 12 classes. We use the ViT-B with a

$16 \times 16$  patch size, pre-trained on ImageNet. We use minibatch Stochastic Gradient Descent (SGD) optimizer [45] with a momentum of 0.9 as the optimizer. The batch size is set to 32. We initialized the learning rate as 0 and linearly warm up to 0.05 after 500 training steps. The results are shown in Table 13 and 14. The methods above the black line are based on CNN architecture, while those under the black line are developed from the Transformer architecture. The ViT-B with positive noise achieves better performance than the existing works. These results show that positive noise can improve model generality, therefore, benefit deep models in domain adaptation tasks.

## References

- [1] Osama K. Al-Shaykh and Russell M. Mersereau. Lossy compression of noisy images. *IEEE Transactions on Image Processing*, 7(12):1641–1652, 1998.
- [2] Wissam A. Albukhanajer, Johann A. Briffa, and Yaochu Jin. Evolutionary multiobjective image feature extraction in the presence of noise. *IEEE Transactions on Cybernetics*, 45(9):1757–1768, 2014.
- [3] Hangbo Bao, Li Dong, and Furu Wei. BEiT: BERT pre-training of image transformers. *arXiv preprint arXiv:2106.08254*, 2021.
- [4] Roberto Benzi, Alfonso Sutera, and Angelo Vulpiani. The mechanism of stochastic resonance. *Journal of Physics A: mathematical and general*, 14(11):L453, 1981.
- [5] George EP Box and David R. Cox. An analysis of transformations. *Journal of the Royal Statistical Society: Series B (Methodological)*, 26(2):211–243, 1964.
- [6] Sebastian Braun, Hannes Gamper, Chandan KA Reddy, and Ivan Tashev. Towards efficient models for real-time deep noise suppression. In *ICASSP 2021-2021 IEEE International Conference on Acoustics, Speech and Signal Processing (ICASSP)*, pages 656–660, 2021.
- [7] Raymond H. Chan, Chung-Wa Ho, and Mila Nikolova. Salt-and-pepper noise removal by median-type noise detectors and detail-preserving regularization. *IEEE Transactions on image processing*, 14(10):1479–1485, 2005.
- [8] Raymond H. Chan, Chung-Wa Ho, and Mila Nikolova. Salt-and-pepper noise removal by median-type noise detectors and detail-preserving regularization. *IEEE Transactions on image processing*, 14(10):1479–1485, 2005.
- [9] Thomas M. Cover. Elements of information theory. *John Wiley & Sons*, 1999.
- [10] Shuhao Cui, Shuhui Wang, Junbao Zhuo, Liang Li, Qingming Huang, and Qi Tian. Towards discriminability and diversity: Batch nuclear-norm maximization under label insufficient situations. *CVPR*, pages 3941–3950, 2020.
- [11] Stéphane d’Ascoli, Hugo Touvron, Matthew Leavitt, Ari Morcos, Giulio Biroli, and Levent Sagun. Convit: Improving vision transformers with soft convolutional inductive biases. *arXiv preprint arXiv:2103.10697*, 2021.
- [12] Mostafa Dehghani, Josip Djolonga, Basil Mustafa, Piotr Padlewski, Jonathan Heek, Justin Gilmer, Andreas Steiner, and et al. Scaling vision transformers to 22 billion parameters. *arXiv preprint arXiv:2302.05442 (2023)*, 2023.
- [13] Jia Deng, Wei Dong, Richard Socher, Li-Jia Li, Kai Li, and Feifei Li. Imagenet: A large-scale hierarchical image database. In *IEEE conference on computer vision and pattern recognition*, pages 248–255, 2009.
- [14] Mingyu Ding, Bin Xiao, Noel Codella, Ping Luo, Jindong Wang, and Lu Yuan. Davit: Dual attention vision transformers. In *In Computer Vision–ECCV 2022: 17th European Conference*, pages 74–92, 2022.
- [15] Alexey Dosovitskiy, Lucas Beyer, Alexander Kolesnikov, Dirk Weissenborn, Xiaohua Zhai, Thomas Unterthiner, Mostafa Dehghani, Matthias Minderer, Georg Heigold, Sylvain Gelly, Jakob Uszkoreit, and Neil Houlsby. An image is worth 16x16 words: Transformers for image recognition at scale. In *arXiv preprint arXiv:2010.11929*, 2020.
- [16] Zhekai Du, Jingjing Li, Hongzu Su, Lei Zhu, and Ke Lu. Cross-domain gradient discrepancy minimization for unsupervised domain adaptation. *CVPR*, pages 3937–3946, 2021.

- [17] Changyong Feng, Hongyue Wang, Naiji Lu, Tian Chen, Hua He, Ying Lu, and Xin M. Tu. Log-transformation and its implications for data analysis. *Shanghai archives of psychiatry*, 26(2):105, 2014.
- [18] Yaroslav Ganin and Victor Lempitsky. Unsupervised domain adaptation by backpropagation. *ICML*, pages 1180–1189, 2015.
- [19] Rafael C. Gonzales and Paul Wintz. *Digital image processing*. Addison-Wesley Longman Publishing Co., Inc., 1987.
- [20] Yves Grandvalet and Yoshua Bengio. Semi-supervised learning by entropy minimization. *NIPS*, pages 211–252, 2004.
- [21] Kaiming He, Xiangyu Zhang, Shaoqing Ren, and Jian Sun. Deep residual learning for image recognition. In *Proceedings of the IEEE conference on computer vision and pattern recognition*, pages 770–778, 2016.
- [22] Roger A. Horn and Johnson Charles R. *Matrix analysis*. Cambridge university press, 2012.
- [23] Norman L. Johnson, Samuel Kotz, and Narayanaswamy Balakrishnan. *Continuous univariate distributions, volume 2*. John wiley & sons, 1995.
- [24] Ravindran Kannan and Achim Bachem. Polynomial algorithms for computing the smith and hermite normal forms of an integer matrix. *siam Journal on Computing*, 8(4):499–507, 1979.
- [25] Solomon Kullback and Richard A. Leibler. On information and sufficiency. *The annals of mathematical statistics*, 22(1):79–86, 1951.
- [26] Ya Le and Xuan Yang. Tiny imagenet visual recognition challenge. *CS 231N 7*, (7), 2015.
- [27] Yann LeCun and Yoshua Bengio. Convolutional networks for images, speech, and time series. *The handbook of brain theory and neural networks*, 3361(10), 1995.
- [28] Shuang Li, Chi Liu, Qiuxia Lin, Binhui Xie, Zhengming Ding, Gao Huang, and Jian Tang. Domain conditioned adaptation network. *AAAI*, pages 11386–11393, 2020.
- [29] Xuelong Li. Positive-incentive noise. *IEEE Transactions on Neural Networks and Learning Systems*, 2022.
- [30] Jian Liang, Dapeng Hu, and Jiashi Feng. Do we really need to access the source data? source hypothesis transfer for unsupervised domain adaptation. *ICML*, pages 6028–6039, 2020.
- [31] Jian Liang, Dapeng Hu, and Jiashi Feng. Domain adaptation with auxiliary target domain-oriented classifier. *CVPR*, pages 16632–16642, 2021.
- [32] Ze Liu, Yutong Lin, Yue Cao, Han Hu, Yixuan Wei, Zheng Zhang, Stephen Lin, and Baining Guo. Swin transformer: Hierarchical vision transformer using shifted windows. In *Proceedings of the IEEE/CVF International Conference on Computer Vision (ICCV)*, 2021.
- [33] Mingsheng Long, Zhangjie Cao, Jianmin Wang, and Michael Jordan. Conditional adversarial domain adaptation. In *Advances in neural information processing systems*, pages 1645–1655, 2018.
- [34] Ilya Loshchilov and Frank Hutter. Decoupled weight decay regularization. *arXiv preprint arXiv:1711.05101*, 2017.
- [35] Marvin Marcus. Determinants of sums. *The College Mathematics Journal*, 2:130–135, 1990.
- [36] Peter McClintock. Can noise actually boost brain power? *Physics World*, 15(7), 2002.
- [37] Alexander McFarlane Mood. *Introduction to the Theory of Statistics*. 1950.
- [38] Toshio Mori and Shoichi Kai. Noise-induced entrainment and stochastic resonance in human brain waves. *Physical review letters*, 88(21), 2002.
- [39] Rich Ormiston, Tri Nguyen, Michael Coughlin, Rana X. Adhikari, and Erik Katsavounidis. Noise reduction in gravitational-wave data via deep learning. *Physical Review Research*, 2(3):033066, 2020.
- [40] J. S. Owotogbe, T. S. Ibiyemi, and B. A. Adu. A comprehensive review on various types of noise in image processing. *int. J. Sci. eng. res*, 10(10):388–393, 2019.
- [41] Sinno Jialin Pan and Qiang Yang. A survey on transfer learning. *IEEE Transactions on knowledge and data engineering*, 22(10):1345–1359, 2009.

- [42] Xingchao Peng, Ben Usman, Neela Kaushik, Judy Hoffman, Dequan Wang, and Kate Saenko. Visda: The visual domain adaptation challenge. *arXiv preprint arXiv:1710.06924*, 2017.
- [43] Lis Kanashiro Pereira, Yuki Taya, and Ichiro Kobayashi. Multi-layer random perturbation training for improving model generalization efficiently. *Proceedings of the Fourth BlackboxNLP Workshop on Analyzing and Interpreting Neural Networks for NLP*, 2021.
- [44] Kamiar Radnosrati, Gustaf Hendeby, and Fredrik Gustafsson. Crackling noise. *IEEE Transactions on Signal Processing*, 68:3590–3602, 2020.
- [45] Sebastian Ruder. An overview of gradient descent optimization algorithms. *arXiv preprint arXiv:1609.04747*, 2016.
- [46] Fabrizio Russo. A method for estimation and filtering of gaussian noise in images. *IEEE Transactions on Instrumentation and Measurement*, 52(4):1148–1154, 2003.
- [47] James P. Sethna, Karin A. Dahmen, and Christopher R. Myers. Crackling noise. *Nature*, 410(6825):242–250, 2001.
- [48] Shai Shalev-Shwartz and Shai Ben-David. *Understanding machine learning: From theory to algorithms*. Cambridge university press, Cambridge, 2014.
- [49] Claude Elwood Shannon. A mathematical theory of communication. *ACM SIGMOBILE mobile computing and communications review*, 5(1):3–55, 2001.
- [50] Jack Sherman and Winifred J. Morrison. Adjustment of an inverse matrix corresponding to changes in the elements of a given column or a given row of the original matrix. *Annals of Mathematical Statistics*, 20, 1949.
- [51] Thomas S Shores. *Applied linear algebra and matrix analysis*. Springer, New York, 2007.
- [52] Jan Sijbers, Paul Scheunders, Noel Bonnet, Dirk Van Dyck, and Erik Raman. Quantification and improvement of the signal-to-noise ratio in a magnetic resonance image acquisition procedure. *Magnetic resonance imaging*, 14(10):1157–1163, 1996.
- [53] Andreas Steiner, Alexander Kolesnikov, Xiaohua Zhai, Ross Wightman, Jakob Uszkoreit, and Lucas Beyer. How to train your vit? data, augmentation, and regularization in vision transformers. In *arXiv preprint arXiv:2106.10270*, 2021.
- [54] Baochen Sun and Kate Saenko. Deep coral: Correlation alignment for deep domain adaptation. *ECCV*, pages 443–450, 2016.
- [55] Chen Sun, Abhinav Shrivastava, Saurabh Singh, and Abhinav Gupta. Revisiting unreasonable effectiveness of data in deep learning era. In *In Proceedings of the IEEE international conference on computer vision*, pages 843–852, 2017.
- [56] Tao Sun, Cheng Lu, Tianshuo Zhang, and Harbin Ling. Safe self-refinement for transformer-based domain adaptation. *Proceedings of the IEEE/CVF Conference on Computer Vision and Pattern Recognition*, pages 7191–7200, 2022.
- [57] Sunil Thulasidasan, Tanmoy Bhattacharya, Jeff Bilmes, Gopinath Chennupati, and Jamal Mohd-Yusof. Combating label noise in deep learning using abstention. In *arXiv preprint arXiv:1905.10964*, 2019.
- [58] Hugo Touvron, Matthieu Cord, Matthijs Douze, Francisco Massa, Alexandre Sablayrolles, and Hervé Jégou. Training data-efficient image transformers & distillation through attention. In *International conference on machine learning*, pages 10347–10357, 2021.
- [59] Zhengzhong Tu, Hossein Talebi, Han Zhang, Feng Yang, Peyman Milanfar, Alan Bovik, and Yinxiao Li. Maxvit: Multi-axis vision transformer. In *In Computer Vision–ECCV 2022: 17th European Conference*, pages 459–479, 2022.
- [60] Ashish Vaswani, Noam Shazeer, Niki Parmar, Jakob Uszkoreit, Llion Jones, Aidan N. Gomez, Łukasz Kaiser, and Illia Polosukhin. Attention is all you need. In *Advances in neural information processing systems*, 2017.
- [61] Hemanth Venkateswara, Jose Eusebio, Shayok Chakraborty, and Sethuraman Panchanathan. Deep hashing network for unsupervised domain adaptation. *CVPR*, pages 5018–5027, 2017.
- [62] Ying Wei, Yu Zhang, Junzhou Huang, and Qiang Yang. Transfer learning via learning to transfer. *ICML*, pages 5085–5094, 2018.

- [63] M. A. Woodbury. Inverting modified matrices. *Statistical Research Group, Memorandum Report 42*, 1950.
- [64] Ruijia Xu, Guanbin Li, Jihan Yang, and Liang Lin. Larger norm more transferable: An adaptive feature norm approach for unsupervised domain adaptation. *ICCV*, pages 1426–1435, 2019.
- [65] Tongkun Xu, Weihua Chen, Fan Wang, Hao Li, and Rong Jin. Cdtrans: Cross-domain transformer for unsupervised domain adaptation. *ICLR*, pages 520–530, 2022.
- [66] Jinyu Yang, Jingjing Liu, Ning Xu, and Junzhou Huang. Tvt: Transferable vision transformer for unsupervised domain adaptation. *WACV*, pages 520–530, 2023.
- [67] Xiaohua Zhai, Alexander Kolesnikov, Neil Houlsby, and Lucas Beyer. Scaling vision transformers. In *Proceedings of the IEEE/CVF Conference on Computer Vision and Pattern Recognition*, pages 12104–12113, 2022.